THE JOURNAL OF COMPARATIVE NEUROLOGY 421:543–569 (2000)

Immunohistochemical Localization of Prostaglandin EP3 Receptor in the Rat Nervous System

KAZUHIRO NAKAMURA,[1]* TAKESHI KANEKO,[2,3] YOKO YAMASHITA,[1] HIROSHI HASEGAWA,[1] HIRONORI KATOH,[1] AND MANABU NEGISHI[1]
[1]Laboratory of Molecular Neurobiology, Graduate School of Biostudies, Kyoto University, Kyoto, Japan 606-8502
[2]Department of Morphological Brain Science, Graduate School of Medicine, Kyoto University, Kyoto, Japan 606-8501
[3]CREST, Japan Science and Technology, Japan

ABSTRACT

The prostaglandin EP3 receptor (EP3R) subtype is believed to mediate large portions of diverse physiologic actions of prostaglandin E_2 in the nervous system. However, the distribution of EP3R protein has not yet been unveiled in the peripheral or central nervous systems. The authors raised a polyclonal antibody against an amino-terminal portion of rat EP3R that recognized specifically the receptor protein. In this study, immunoblotting analysis with this antibody showed several immunoreactive bands with different molecular weights in rat brain extracts and in membrane fractions of recombinant EP3R-expressing culture cells, and treatment with *N*-glycosidase shifted those immunoreactive bands to an apparently single band with a lower molecular weight, suggesting that EP3R proteins are modified posttranslationally with carbohydrate moieties of various sizes. The authors performed immunohistochemical investigation of EP3R in the rat brain, spinal cord, and peripheral ganglia by using the antibody. EP3R-like immunoreactivity was observed in many and discrete regions of the rostrocaudal axis of the nervous system. The signals were particularly strong in the anterior, intralaminar, and midline thalamic nuclear groups; the median preoptic nucleus; the medial mammillary nucleus; the superior colliculus; the periaqueductal gray; the lateral parabrachial nucleus; the nucleus of the solitary tract; and laminae I and II of the medullary and spinal dorsal horns. Sensory ganglia, such as the trigeminal, dorsal root, and nodose ganglia, contained many immunopositive neurons. Neuronal cells in the locus coeruleus and raphe nuclei exhibited EP3R-like immunoreactivity. This suggests that EP3R plays regulatory roles in the noradrenergic and serotonergic monoamine systems. Autonomic preganglionic nuclei, such as the dorsal motor nucleus of the vagus nerve, the spinal intermediolateral nucleus, and the sacral parasympathetic nucleus, also contained neuronal cell bodies with the immunoreactivity, implying modulatory functions of EP3R in the central autonomic nervous system. The characteristic distribution of EP3R provides valuable information on the mechanisms for various physiologic actions of prostaglandin E_2 in the central and peripheral nervous systems. J. Comp. Neurol. 421:543–569, 2000.

Indexing terms: prostaglandin E_2; immunohistochemistry; *N*-linked glycosylation; immunoblotting; monoamine system; autonomic nervous system

Prostaglandin (PG) E_2 is known to have various physiologic functions in the nervous system, such as fever induction (Stitt, 1986; Blatteis and Sehic, 1998), pain modulation (Ferreira, 1972; Ferreira et al., 1973, 1978), regulation of vasopressin and luteinizing hormone-releasing hormone secretion (Vilhardt and Hedqvist, 1970; Ojeda et al., 1982), regulation of food intake (Scaramuzzi et al., 1971), and sleep-wake regulation (Onoe et al., 1992; Hayaishi and Matsumura, 1995). PGE_2 exerts

Grant sponsor: Ministry of Education, Science, Sports and Culture of Japan; Grant numbers: 10470482 and 11780579; Grant sponsor: Asahi Glass Research Foundation; Grant sponsor: Mochida Memorial Foundation for Medical and Pharmaceutical Research.

*Correspondence to: Kazuhiro Nakamura, Laboratory of Molecular Neurobiology, Graduate School of Biostudies, Kyoto University, Sakyo-ku, Kyoto, Japan 606-8502. E-mail: nkazuhir@pharm.kyoto-u.ac.jp

Received 16 September 1999; Revised 30 November 1999; Accepted 9 February 2000

these diverse actions through specific cell-surface receptors. The PGE receptors were divided pharmacologically into four subtypes (EP1, EP2, EP3, and EP4) on the basis of their responses to various agonists and antagonists. Molecular cloning and biochemical approaches revealed that they belong to a rhodopsin-type receptor superfamily and are coupled to various signal-transduction systems (for review, see Negishi et al., 1995). To clarify the mechanisms for those PGE_2 actions, several histochemical studies were performed in the central nervous system (CNS). However, most of the studies focused on cyclooxygenases—rate-limiting enzymes in the biosynthesis of PGs (Breder et al., 1992, 1995)—and demonstrated that cyclooxygenase-2 was induced in discrete populations of neuronal cells by synaptic stimuli (Yamagata et al., 1993). Those studies contributed to an explanation of the

Abbreviations

3V	third ventricle
4V	fourth ventricle
ac	anterior commissure
ACo	anterior cortical amygdaloid nucleus
AD	anterodorsal thalamic nucleus
AH	anterior hypothalamic area
Am	ambiguus nucleus
AM	anteromedial thalamic nucleus
AP	area postrema
APt	anterior pretectal nucleus
Aq	aqueduct
Ar	arcuate nucleus
AT	anterior tegmental nucleus
AV	anteroventral thalamic nucleus
BL	basolateral amygdaloid nucleus
BM	basomedial amygdaloid nucleus
CA1–CA3	fields CA1–3 of Ammon's horn
Ce	central amygdaloid nucleus
Cf	cuneiform nucleus
CL	central lateral thalamic nucleus
CM	central medial thalamic nucleus
CP	caudate-putamen
Cu	cuneate nucleus
CVL	caudoventrolateral reticular nucleus
DG	dentate gyrus
DH	spinal dorsal horn
DMc	compact part of the dorsomedial hypothalamic nucleus
DMd	dorsal part of the dorsomedial hypothalamic nucleus
DMV	dorsal motor nucleus of the vagus nerve
DpG	deep gray layer of the superior colliculus
DpW	deep white layer of the superior colliculus
DR	dorsal raphe nucleus
DT	dorsal tegmental nucleus
EPi	endopiriform nucleus
f	fornix
fr	fasciculus retroflexus
Gia	alpha part of the gigantocellular reticular nucleus
Giv	ventral part of the gigantocellular reticular nucleus
GP	globus pallidus
Hy	hypoglossal nucleus
IC	inferior colliculus
IML	intermediolateral nucleus
InG	intermediate gray layer of the superior colliculus
InW	intermediate white layer of the superior colliculus
IOC	inferior olivary complex
IP	interpeduncular nucleus
LA	lateral amygdaloid nucleus
LC	locus coeruleus
LD	laterodorsal thalamic nucleus
LG	lateral geniculate nucleus
Li	linear nucleus of the raphe
LP	lateral posterior thalamic nucleus
LPB	lateral parabrachial nucleus
LS	lateral septal nucleus
LV	lateral ventricle
MDl	lateral part of the mediodorsal thalamic nucleus
Me	medial amygdaloid nucleus
MG	medial geniculate nucleus
MHb	medial habenular nucleus
Mm	median part of the medial mammillary nucleus
MnPO	median preoptic nucleus
MnR	median raphe nucleus
MPB	medial parabrachial nucleus
MPO	medial preoptic area
mt	mammillotegmental tract
oc	optic chiasm
Op	optic nerve layer of the superior colliculus
OPt	olivary pretectal nucleus
OT	nucleus of the optic tract
P	pontine nuclei
Pa	paraventricular hypothalamic nucleus
PAG	periaqueductal gray
PC	paracentral thalamic nucleus
Pe	periventricular hypothalamic nucleus
Pef	perifornical nucleus
Pf	parafascicular thalamic nucleus
PH	posterior hypothalamic area
Pir	piriform cortex
PLCo	posterolateral cortical amygdaloid nucleus
PMCo	posteromedial cortical amygdaloid nucleus
PMd	dorsal part of the premammillary nucleus
PnR	pontine raphe nucleus
Po	posterior thalamic nuclear group
PRa	alpha part of the parvicellular reticular nucleus
PS	parastrial nucleus
PT	paratenial thalamic nucleus
PTR	pontine tegmental reticular nucleus
PV	paraventricular thalamic nucleus
R	red nucleus
Re	reuniens thalamic nucleus
Rh	rhomboid thalamic nucleus
RMg	raphe magnus nucleus
ROb	raphe obscurus nucleus
RPa	raphe pallidus nucleus
RRF	retrorubral field
RS	retrosplenial cortex
RVL	rostroventrolateral reticular nucleus
SCh	suprachiasmatic nucleus
SF	septofimbrial nucleus
SG	suprageniculate thalamic nucleus
Sm	submedius (or gelatinosus) thalamic nucleus
SM	supramammillary nucleus
SNc	compact part of the substantia nigra
SNr	reticular part of the substantia nigra
SO	supraoptic nucleus
SOC	superior olivary complex
Sol	nucleus of the solitary tract
SP	sacral parasympathetic nucleus
SPf	subparafascicular thalamic nucleus
SubC	subcoeruleus nucleus
SubI	subincertal nucleus
SuG	superficial gray layer of the superior colliculus
VA	ventral anterior thalamic nucleus
Vc	caudal part of the spinal trigeminal nucleus
VH	spinal ventral horn
Vi	interpolar part of the spinal trigeminal nucleus
VL	ventral lateral thalamic nucleus
VM	ventral medial thalamic nucleus
Vmo	motor trigeminal nucleus
Vo	oral part of the spinal trigeminal nucleus
Vp	principal sensory trigeminal nucleus
VPL	ventral posterolateral thalamic nucleus
VPM	ventral posteromedial thalamic nucleus
VT	ventral tegmental nucleus
Xi	xiphoid thalamic nucleus
ZI	zona incerta
Zo	zonal layer of the superior colliculus

PG production mechanism in the CNS, whereas histochemical approaches to the PGE receptors have almost never been performed.

Among the PGE receptor subtypes, the EP3 receptor (EP3R) has been the best characterized and has been reported to be involved in contraction of the uterus (Krall et al., 1984), inhibition of gastric acid secretion (Chen et al., 1988), lipolysis in the adipose tissue (Richelsen and Beck-Nielsen, 1984), and sodium and water reabsorption in the kidney tubules (Garcia-Perez and Smith, 1984). These various actions of EP3R have been thought to be induced by inhibition of adenylate cyclase or stimulation of Ca^{2+} mobilization (Negishi et al., 1995). In addition to peripheral actions, EP3R also has been shown to have physiologic roles in the nervous system, such as fever induction (Ushikubi et al., 1998), pain modulation (Kumazawa et al., 1993; Minami et al., 1994; Oka et al., 1997), and regulation of the autonomic nervous system (Mantelli et al., 1991; Molderings et al., 1992, 1994; Yokotani et al., 1996; Reinheimer et al., 1998; Spicuzza et al., 1998). However, the neuronal mechanisms for the diverse functions of EP3R remain obscure. Details of the distribution of the receptor in the nervous system would provide a great deal of information on those mechanisms. Although several reports have indicated PGE_2 binding sites in the mammalian brain using a radiolabelled ligand (Watanabe et al., 1988; Matsumura et al., 1990, 1992) and an anti-PGE_2 antibody (Fujimoto et al., 1992), it has not yet been identified which subtypes of PGE receptors are expressed in those sites.

We previously showed the distribution of mRNA for EP3R in the mouse nervous system by using in situ hybridization (Sugimoto et al., 1994). Recently, we produced a polyclonal antibody specific to rat EP3R and revealed the immunocytochemical localization of the receptor protein in the rat hypothalamus (Nakamura et al., 1999). In the current study, we examined in detail the distribution of immunoreactivity with the antibody against EP3R and mapped the function sites of EP3R in the rostrocaudal axis of the rat central and peripheral nervous systems.

MATERIALS AND METHODS

Antibody production and purification

The production, purification, and characterization of the antibody against rat EP3R have been reported previously (Nakamura et al., 1999). Briefly, antisera were raised in rabbits by immunization with a bacterially expressed glutathione-*S*-transferase fused with an N-terminal part of rat EP3R (residues 2–28; A G V W A P E H S V E A H S N Q S S A A D G C G S V S; single-letter amino acid code), which is a common portion to known three splice variants, EP3α, EP3β, and EP3γ. A polyclonal antibody was purified from the antisera with a Protein G Superose column (Pharmacia, Uppsala, Sweden) followed by affinity purification with an AffiGel 15 column (BioRad, Hercules, CA) conjugated with a synthetic peptide (TANA Laboratories, Houston, TX) corresponding to residues 2–28 of rat EP3R. The antibody eluted from the affinity column with 0.1 M glycine-HCl, pH 2.5, showed high reactivity and specificity to rat EP3R and was used in this study.

Immunopurification of EP3R protein

Because the content of endogenous EP3R protein in rat brains was too low to be detected with immunoblotting analysis, immunopurification of the receptor protein was carried out as described previously (Nakamura et al., 1999). In brief, rat brains were homogenized with 9 volumes of 50 mM Tris-HCl, pH 7.4, containing 0.5% Triton X-100, 5 mM ethylenediaminetetraacetic acid, 0.2 mM phenylmethylsulfonyl fluoride, 1 μg/ml aprotinin, 1 μg/ml leupeptin, and 0.1 mM benzamidine followed by centrifugation at 100,000 × *g* for 1 hour. The supernatant was applied to an AffiGel 10 column (BioRad) conjugated with the affinity-purified antibody (1.6 mg antibody/1 ml gel). After a vigorous wash with 1 M NaCl containing 1% Tween 20, bound protein was eluted from the column with 0.1 M glycine-HCl, pH 2.5, containing 1% Tween 20, and the eluate was subjected to deglycosylation.

Deglycosylation and immunoblotting

Membrane fractions from rat EP3β receptor-expressing COS-7 green monkey kidney cells were prepared by using the same method described previously (Nakamura et al., 1999). The eluate from the antibody column (180 ng protein) or membrane fractions of the COS-7 cells (77 μg protein) were boiled for 5 minutes in 75 μl of 1% sodium dodecyl sulfate (SDS) solution containing 1% 2-mercaptoethanol. After it was placed at room temperature for 10 minutes, the solution was mixed with 25 μl of 0.2 mM potassium phosphate buffer, pH 7.0, containing 2% Nonidet P-40. To 50 μl of this sample, 10 μl of 200 units/ml *N*-glycosidase F (Boehringer Mannheim, Indianapolis, IN) were added, and the mixture was incubated at 37°C for 2 hours. Instead of the enzyme, the same volume of water was added to untreated samples. After the incubation, all the protein samples were subjected to electrophoresis in a 10% polyacrylamide gel with SDS and transferred onto a polyvinylidene difluoride membrane. After blocking with 3% skim milk, the membrane was incubated with 1.4 μg/ml rabbit anti-rat EP3R antibody and then with horseradish peroxidase-conjugated goat anti-rabbit immunoglobulin G (IgG) antibody (dilution, 1:2,000; BioSource International, Camarillo, CA) followed by detection with an enhanced chemiluminescence system (Amersham, Buckinghamshire, United Kingdom). In a detailed analysis of electrophoretic mobility, a 12.5% polyacrylamide gel containing 6 M urea was used for the electrophoresis, and the horseradish peroxidase activity was detected with a tetramethylbenzidine substrate kit (Vector Laboratories, Burlingame, CA).

Immunohistochemistry

Ten male Sprague-Dawley rats (body weight, 200–400 g; SLC Japan, Hamamatsu, Japan) were deeply anesthetized with intraperitonial administration of pentobarbital (50 mg/kg body weight) and were fixed by transcardial perfusion with 300 ml of a cold fixative containing 4% paraformaldehyde in 0.1 M phosphate buffer, pH 7.4. The brain and spinal cord were removed, cut into several blocks, postfixed in the same fixative at 4°C for 8 hours, and then saturated with 0.1 M phosphate buffer containing 25% (weight/volume) sucrose at 4°C for 48 hours. The blocks were cut into 40-μm-thick frontal sections on a cryostat at −20°C. The sections were collected consecutively into six bottles; six series of sections were obtained from each rat. The trigeminal, dorsal root, nodose, superior cervical, and stellate ganglia also were removed, postfixed, cryoprotected, and cut into 20-μm-thick frozen sections. The sections of the ganglia were mounted onto poly-L-lysine-coated slides, air-dried briefly, and then

rehydrated in 50 mM phosphate-buffered saline (PBS), pH 7.3.

The sections were incubated overnight at room temperature with 1 μg/ml affinity-purified rabbit antibody to rat EP3R in PBS containing 0.3% Triton X-100, 0.25% λ-carrageenan, and 0.5% normal donkey serum. After a rinse in PBS containing 0.3% Triton X-100, the sections were incubated for 1 hour with 10 μg/ml biotinylated donkey antibody to rabbit IgG (Chemicon, Temecula, CA). The sections were rinsed again and reacted for 1 hour with avidin-biotin-peroxidase complex (1:50; Elite ABC Kit; Vector Laboratories). After a thorough wash of the sections in PBS, bound peroxidase finally was visualized by incubation for 20–40 minutes with 0.02% 3,3′-diaminobenzidine tetrahydrochloride (Dojindo, Kumamoto, Japan) and 0.001% hydrogen peroxide in 50 mM Tris-HCl, pH 7.6. In control experiments, the primary antibody was preincubated with a 16-fold (molar ratio) excess amount of the fusion protein used as the immunogen for 1 hour at room temperature prior to the incubation of sections. For the study of cytoarchitecture, one of the rostrocaudal series of the immunostained sections was counterstained with cresyl violet. The anatomic nomenclature of Paxinos and Watson (1998) was adopted in most regions of the nervous system. Data and figures are from five representative rats. No significant differences in immunostaining patterns were found between animals. All experimental procedures in the current study were approved by the Animal Care and Use Committee at the Graduate School of Biostudies at Kyoto University, Japan.

RESULTS

Characterization of EP3R protein

In our previous study with an antibody to rat EP3R (Nakamura et al., 1999), we performed immunoblotting of the rat brain, kidney, and EP3R-expressing COS-7 cells to characterize the antibody and detected several immunoreactive bands with different molecular weights, all of which were absorbed by preincubation of the antibody with the immunogen, indicating that the antibody specifically recognizes EP3R protein. The heterogeneity of the immunoreactive bands was attributed to various sizes of carbohydrate moieties that were added posttranslationally onto the receptor protein molecules, because rat EP3R has two potential sites for *N*-linked glycosylation in the extracellular domains (Takeuchi et al., 1993, 1994; Kitanaka et al., 1996). Here, we examined this possibility. Immunoblotting analysis was performed to detect glycosylated EP3R protein in the rat brain or in the COS-7 cells transiently expressing rat EP3β receptor (Fig. 1A). Because we could not detect any immunoreactivity in crude extracts of rat brains (Nakamura et al., 1999), the extracts were applied to an anti-EP3R antibody-conjugated column to increase the concentration of the endogenous receptor protein. In the eluate from the column (Fig. 1A, lane 1), the antibody showed major immunoreactive bands at around 50 kDa (Fig. 1A, arrow) and a minor immunoreactive band at about 39 kDa. Treatment of the eluate with *N*-glycosidase shifted these immunoreactive bands to an apparently single band at about 33 kDa (Fig. 1A, lane 2, arrowhead). In membrane fractions of rat EP3β receptor-expressing COS-7 cells, major and broad immunoreactive bands were detected at 60–100 kDa, and three minor

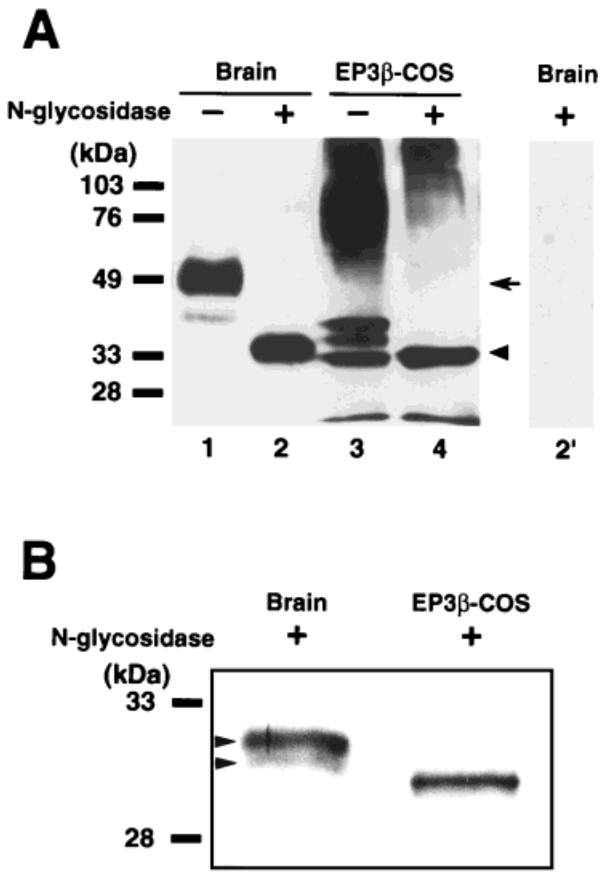

Fig. 1. Characterization of the prostaglandin EP3 receptor (EP3R) protein in the rat brain and EP3R-expressing COS-7 cells by deglycosylation and immunoblotting. **A:** Protein immunopurified from rat brains (24 ng/lane) was incubated in a buffer without (lane 1) or with (lane 2) *N*-glycosidase. Membrane protein of rat EP3β receptor-expressing COS-7 cells (13 μg/lane) also was (lane 4) or was not (lane 3) subjected to deglycosylation. No immunoreactivity was detected after preincubation of the anti-EP3R antibody used in immunoblotting with an excess amount of the antigen (lane 2′). An arrow indicates the major immunoreactive bands in lane 1. An arrowhead indicates the apparently single band in lane 2. Immunoreactive bands seen at the bottom of lanes 3 and 4 indicate the front lines of the electrophoresis. **B:** After the deglycosylation, the protein immunopurified from rat brains (left) or the membrane fractions of the EP3β receptor-expressing COS-7 cells (right) was analyzed with higher resolution by electrophoresis in a urea-containing polyacrylamide gel. Arrowheads indicate the two adjacent immunoreactive bands.

immunoreactive bands were seen at about 39, 37, and 33 kDa (Fig. 1A, lane 3), all of which were also shifted to about 33 kDa by the *N*-glycosidase treatment (Fig. 1A, lane 4). The band shifts by the deglycosylation indicate that all of the immunoreactive bands with different molecular weights are derived from identical protein molecules. *N*-glycosidase-insensitive immunoreactive bands were observed above 100 kDa in the lanes of the COS-7 cells (Fig. 1A, lanes 3 and 4), which probably reflected oligomerization of the receptor protein molecules as reported in adrenaline β_2 and dopamine D_3 receptors (Hebert et al., 1996; Nimchinsky et al., 1997). All of the immunoreactivity described here was absorbed completely

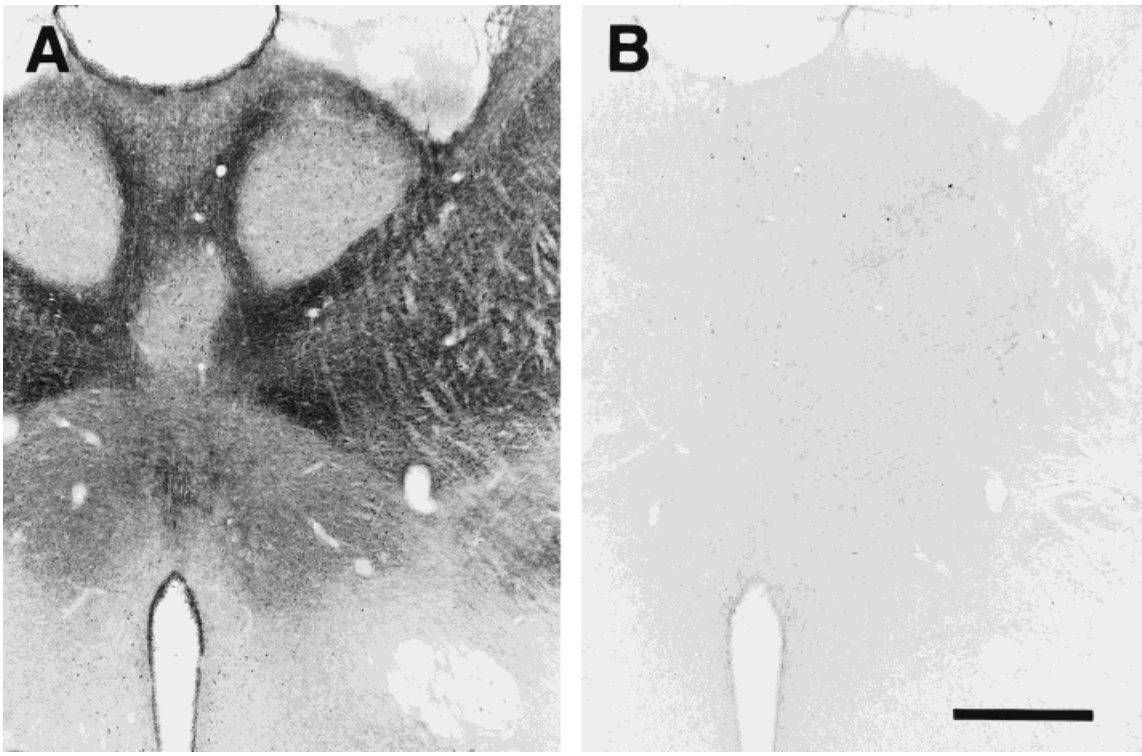

Fig. 2. Preabsorption experiment to assess the specificity of immunoperoxidase staining with the anti-EP3R antibody. **A:** Intense immunoreactivity was detected in the anterior thalamic nuclear group by using the anti-EP3R antibody. **B:** Signals were not observed at all when the primary antibody was preincubated with an excess amount of the immunogen. Note that the immunoreactivity that was observed not only in the brain parenchyma but also in the ependyma was absorbed clearly. Scale bar = 500 μm.

by preincubation of the primary antibody with an excess amount of the fusion protein used as the immunogen (Fig. 1A, lane 2′). These results further strongly supported the antibody's specificity to rat EP3R.

In Figure 1B, the deglycosylated proteins were electrophoresed in a urea-containing polyacrylamide gel to analyze the electrophoretic mobilities with higher resolution. In the lane of the rat brain (Fig. 1B, left), we detected two adjacent immunoreactive bands at around 31 kDa (Fig. 1B, arrowheads), whereas only a single band was observed at 30 kDa in the lane of the COS-7 cells expressing rat EP3β receptor (Fig. 1B, right).

Distribution of EP3R in the nervous system

EP3R-like immunoreactivity (EP3R-LI) was distributed widely in the central and peripheral nervous systems, although the olfactory bulb and cerebellum did not show any immunoreactivity. EP3R-LI was observed mainly in neurons. However, intense immunoreactivity also was localized in the ependymal cells surrounding the lateral ventricle, the third and fourth ventricles, and the aqueduct (Figs. 2A, 4A–O, 8C, arrows). Other glial cells and nonneuronal cells of the choroid plexus, meninges, and blood vessels were not immunostained at all. In control immunostaining experiments, preincubation of the primary antibody with an excess amount of the immunogen abolished EP3R-LI (Fig. 2B) in all areas of the nervous system, demonstrating the high specificity of the immunostaining.

EP3R-LI was seen rather diffusely in neuropil of most regions of the brain and spinal cord by immunoperoxidase staining with the antibody (Fig. 3A–C), although neuronal cell bodies with EP3R-LI were observed clearly in some regions. Internal standards were employed to evaluate the intensity of EP3R-LI semiquantitatively: The immunoreactivity in neuropil was intense (+++) in the paraventricular thalamic nucleus (Fig. 3A), moderate (++) in the zonal and superficial gray layers of the superior colliculus (Fig. 3B), weak (+) in the dorsal lateral geniculate nucleus (Fig. 3C), and negative (−) in the paratenial thalamic nucleus (Fig. 3D). The distribution pattern of EP3R-LI is summarized in Table 1 in terms of the intensity of EP3R-LI in neuropil. Table 1 also lists the regions in which neuronal cell bodies with EP3R-LI were visible.

Cerebral cortex. Layer V showed EP3R-LI in neuropil: The immunoreactivity was moderate to weak in the prelimbic, infralimbic, cingulate, retrosplenial, insular, ectorhinal, and perirhinal cortices (Figs. 4I, 5C,D) and weak in the superficial zone of layer V of the neocortex (Fig. 5A). However, the deep zone of layer V of the neocortex showed no EP3R-LI. Moderate or weak EP3R-LI was observed in the neuropil of layer I of the insular, ectorhinal, and perirhinal cortices (Fig. 5D), and weak immunoreactivity was detected in the neuropil of layer I of the prelimbic, infralimbic, cingulate, and retrosplenial cortices (Fig. 5C). Neuronal cell bodies exhibiting weak EP3R-LI were scattered in layer VI of the neocortex, the insular cortex, the ectorhinal cortex, and the perirhinal

TABLE 1. Distribution of Prostaglandin EP3 Receptor Immunoreactivity in the Rat Nervous System

Sites	Neuropil[1]	Cell bodies[2]
Olfactory bulb	−	−
Neocortex		
Layers I–IV and V (deep)	−	−
Layer V (superficial)	+	−
Layer VI	−	+ (scattered)
Prelimbic, infralimbic, cingulate, and retrosplenial cortices		
Layer I	+	−
Layers II–IV and VI	−	−
Layer V	+~++	−
Insular, ectorhinal, and perirhinal cortices		
Layers I and V	+~++	−
Layers II–IV	−	−
Layer VI	−	+ (scattered)
Piriform cortex		
Layers I and III	+	−
Layer II	−	−
Entorhinal cortex		
Layers I–III	−	−
Layers IV–VI	+~++	−
Ammon's horn		
Stratum oriens	−	+ (scattered)
Pyramidal cell layer	−	+
Stratum radiatum	−	+ (scattered)
Stratum lacunosum-moleculare	+	−
Dentate gyrus		
Molecular layer	+	−
Granule cell layer	−	+
Polymorph layer	−	+ (scattered)
Subiculum	+	−
Postsubiculum	+	−
Presubiculum	−	−
Parasubiculum	−	−
Septal region		
Lateral septal nucleus		
Dorsal part	−	−
Ventral part	+	+
Intermediate part	+~++	+
Medial septal nucleus	−	−
Septofimbrial nucleus	+	+
Nucleus of the diagonal band	−	−
Basal ganglia		
Caudate-putamen	+	−
Accumbens nucleus	+~++	−
Globus pallidus	+	−
Islands of Calleja	+	−
Endopiriform nucleus	+~++	−
Entopeduncular nucleus	−	−
Claustrum	−	−
Amygdala		
Anterior cortical amygdaloid nucleus	+~++	−
Posteromedial cortical amygdaloid nucleus		
Rostral part	+~++	−
Caudal part	−	−
Posterolateral cortical amygdaloid nucleus		
Rostral part	+	−
Caudal part	−	−
Lateral amygdaloid nucleus	+~++	−
Basolateral amygdaloid nucleus	+	−
Medial amygdaloid nucleus	+	−
Basomedial amygdaloid nucleus	+~++	−
Central amygdaloid nucleus	+	−
Anterior amygdaloid area	±	−
Preoptic region and hypothalamus		
Medial preoptic area	++~+++	+
Lateral preoptic area	−	−
Median preoptic nucleus	+++	+
Anteroventricular periventricular nucleus	−	−
Ventromedial preoptic nucleus	−	−
Parastrial nucleus	+++	−
Suprachiasmatic nucleus	−	−
Supraoptic nucleus	−	−
Anterior hypothalamic area		
Anterior part	+	−
Posterior part	+	+ (scattered)
Periventricular nucleus	+~++	+
Paraventricular hypothalamic nucleus	+~++	−
Dorsal hypothalamic area	+	+ (scattered)
Dorsomedial hypothalamic nucleus		
Compact part	+++	−
Dorsal and ventral parts	+	+ (scattered)
Perifornical nucleus	+	+ (scattered)
Subincertal nucleus	+	+ (scattered)
Posterior hypothalamic area	+	+ (scattered)
Arcuate nucleus		
Lateroposterior part	+	+
Other parts	−	−
Premammillary nucleus		
Dorsal part	++~+++	−
Ventral part	−	−
Supramammillary nucleus		
Dorsal part	−	−
Ventral part	++~+++	−
Medial mammillary nucleus		
Median part	+++	−
Medial and lateral parts	+	−
Thalamus		
Anteroventral nucleus	++~+++	−
Anteromedial nucleus	++~+++	+
Anterodorsal nucleus	+~++	−
Mediodorsal nucleus		
Lateral part	+	+
Medial and central parts	−	−
Ventral anterior nucleus	+	+
Ventral lateral nucleus	+	+
Ventral medial nucleus	+	+
Ventral posteromedial nucleus	+	−
Ventral posterolateral nucleus	+	−
Laterodorsal nucleus		
Rostral part	+++	+
Caudal part	++	+
Lateral posterior nucleus		
Mediocaudal part	++	−
Other parts	+~++	+
Posterior nuclear group	+	+
Central lateral nucleus	+~++	+
Central medial nucleus	++~+++	+
Paracentral nucleus	++~+++	+
Parafascicular nucleus	+	+
Subparafascicular nucleus	+	+
Paraventricular nucleus	+++	−
Intermediodorsal nucleus	+~++	+
Paratenial nucleus	−	−
Interanterodorsal nucleus	+++	+
Interanteromedial nucleus	+++	+
Rhomboid nucleus		
Rostral part	−	−
Caudal part	++~+++	+
Reuniens nucleus	+	+
Xiphoid nucleus	++~+++	+
Submedius (or gelatinosus) nucleus	−	−
Dorsal lateral geniculate nucleus	+	−
Ventral lateral geniculate nucleus	+~++	−
Suprageniculate nucleus	+	+
Medial geniculate nucleus	+	+
Habenula		
Medial habenular nucleus		
Lateral part	+++	+ (scattered)
Medial part	−	−
Lateral habenular nucleus	−	−
Zona incerta		
Rostral part	++	−
Intermediate and caudal parts	−	−
Pretectum		
Nucleus of the optic tract	+	−
Anterior pretectal nucleus	−	−
Medial pretectal nucleus	−	−
Olivary pretectal nucleus	+	−
Posterior pretectal nucleus	−	−
Precommissural nucleus	−	−
Superior colliculus		
Zonal layer	++	−
Superficial gray layer	++	−
Optic nerve layer	+	−
Intermediate gray layer	−	−
Intermediate white layer	−	−
Deep gray layer	+~++	−
Deep white layer	−	−
Periaqueductal gray		
Dorsolateral part		
Anterior one-third	+	+
Posterior two-thirds	++	−
Other parts		
Rostral portion	−	−
Caudal portion	+	−
Edinger-Westphal nucleus	−	−
Oculomotor nucleus	−	−

Table 1. (Continued)

Sites	Neuropil[1]	Cell bodies[2]	Sites	Neuropil[1]	Cell bodies[2]
Trochlear nucleus	−	−	Raphe magnus nucleus	++	+
Terminal nuclei of the accessory optic tract	−	−	Raphe obscurus nucleus	++	+
			Raphe pallidus nucleus	++	+
Retrorubral field	+~++	−	Gigantocellular reticular nucleus		
Ventral tegmental area	−	−	Alpha and ventral parts		
Substantia nigra	−	−	Lateral portion	++	+
Red nucleus	−	−	Medial and intermediate portions	−	−
Inferior colliculus	−	−			
Cuneiform nucleus	+~++	−	Other parts	−	−
Mesencephalic trigeminal nucleus	−	−	Area postrema	±	−
Rostral linear nucleus of the raphe	+	+ (scattered)	Cochlear nuclei	−	−
Caudal linear nucleus of the raphe	−	−	Abducens nucleus	−	−
Dorsal raphe nucleus	++	+	Facial nucleus	−	−
Median raphe nucleus	+~++	+	Vestibular nuclei	−	−
Anterior tegmental nucleus	+	−	Hypoglossal nucleus	−	−
Ventral tegmental nucleus	+	−	Ambiguus nucleus		
Interpeduncular nucleus			Rostral part	++	−
Dorsomedial and dorsolateral subnuclei	+~++	−	Caudal part	−	−
			External cuneate nucleus	−	−
Other subnuclei	−	−	Cuneate nucleus	−	−
Lateral parabrachial nucleus			Gracile nucleus	−	−
External, central, and crescent parts	++~+++	−	Inferior olivary complex		
			Principal nucleus	+	−
Dorsal part	++	−	Other nuclei	−	−
Ventral and internal parts	−	−	Prepositus hypoglossal nucleus	−	−
Medial parabrachial nucleus			Lateral reticular nucleus	−	−
Rostral part	−	−	Rostroventrolateral reticular nucleus	+	+ (scattered)
Caudal part	+	+	Caudoventrolateral reticular nucleus	+	+ (scattered)
Locus coeruleus	++	+ (scattered)	Spinal trigeminal nucleus		
Subcoeruleus nucleus	−	+ (scattered)	Caudal part		
Pontine raphe nucleus	+	+	Lamina I	+	−
Pontine tegmental reticular nucleus	−	+ (scattered)	Lamina II	++~+++	−
Dorsal tegmental nucleus	−	−	Other laminae	−	−
Superior olivary complex	−	−	Other parts	−	−
Nucleus of the trapezoid body	−	−	Spinal cord		
Motor trigeminal nucleus	−	−	Lamina I	+	−
Principal sensory trigeminal nucleus	−	−	Lamina II	++~+++	−
Pontine nuclei	−	−	Other laminae	−	−
Cerebellum	−	−	Intermediolateral nucleus	++	+ (scattered)
Nucleus of the solitary tract			Sacral parasympathetic nucleus	++	+
Commissural part	+++	−	Trigeminal ganglion	+	+
Medial part	++~+++	−	Dorsal root ganglion	+	+
Intermediate part	++~+++	±	Nodose ganglion	+	+
Ventrolateral part	+	−	Superior cervical ganglion	+	+
Dorsal motor nucleus of the vagus nerve	++	+ (scattered)	Stellate ganglion	+	+

[1]The intensity of prostaglandin EP3 receptor immunoreactivity in neuropil was scored visually by using the internal standard (see Fig. 3): +++, intense; ++, moderate; +, weak; −, negative.
[2]The regions where immunostained neuronal cell bodies were or were not found are shown by + and −, respectively. The regions where scattered immunopositive neuronal cell bodies were observed are denoted by (scattered).

cortex (Fig. 5B), although no cell bodies with EP3R-LI were seen in the prelimbic, infralimbic, cingulate, or retrosplenial cortices. EP3R-LI was moderate to weak in the neuropil of layers IV–VI of the entorhinal cortex and weak in the neuropil of layers I and III of the piriform cortex (Fig. 5E). However, EP3R-LI was not detected in layers I–III of the entorhinal cortex or in layer II of the piriform cortex. Cell bodies with immunoreactivity were not observed in the entorhinal or piriform cortices.

Hippocampus. Weak EP3R-LI was seen in neuronal cell bodies of Ammon's horn (Fig. 4C–E). Many pyramidal neurons exhibited immunoreactivity, and a few neuronal cells with EP3R-LI were scattered in the stratum oriens and stratum radiatum. Neuropil was weakly immunostained in the stratum lacunosum-moleculare. In the dentate gyrus (Fig. 4E,G,H), weak EP3R-LI was observed in many neuronal cells of the granule cell layer and in some neuronal cells dispersed in the polymorph layer. The molecular layer exhibited weak EP3R-LI in the neuropil. EP3R-LI also was weak in the neuropil of the subiculum and postsubiculum, but no immunoreactivity was detected in the presubiculum or parasubiculum.

Amygdala. EP3R-LI in neuropil was moderate to weak in the anterior cortical amygdaloid nucleus and in the rostral part of the posteromedial cortical amygdaloid nucleus, and it was weak in the rostral part of the posterolateral cortical amygdaloid nucleus (Figs. 4F–H, 5E). However, no EP3R-LI was detected in the caudal parts of the posteromedial and posterolateral cortical amygdaloid nuclei. Moderate or weak EP3R-LI was observed in the neuropil of the lateral and basomedial amygdaloid nuclei (Fig. 5E,F). Weak EP3R-LI was seen in the neuropil of the basolateral, medial, and central amygdaloid nuclei (Fig. 5E). EP3R-LI in the anterior amygdaloid area was weak or negative. No cell bodies with EP3R-LI could be detected throughout the amygdaloid body.

Basal ganglia and septal and basal forebrain regions. Moderate or weak EP3R-LI was detected in the neuropil of the endopiriform nucleus (Fig. 5E), although the claustrum showed no immunoreactivity. EP3R-LI was moderate to weak in the neuropil of the accumbens nucleus and was weak in the neuropil of the caudate-putamen, globus pallidus, and islands of Calleja (Fig. 4A,B). Immunoreactivity was not observed in the entope-

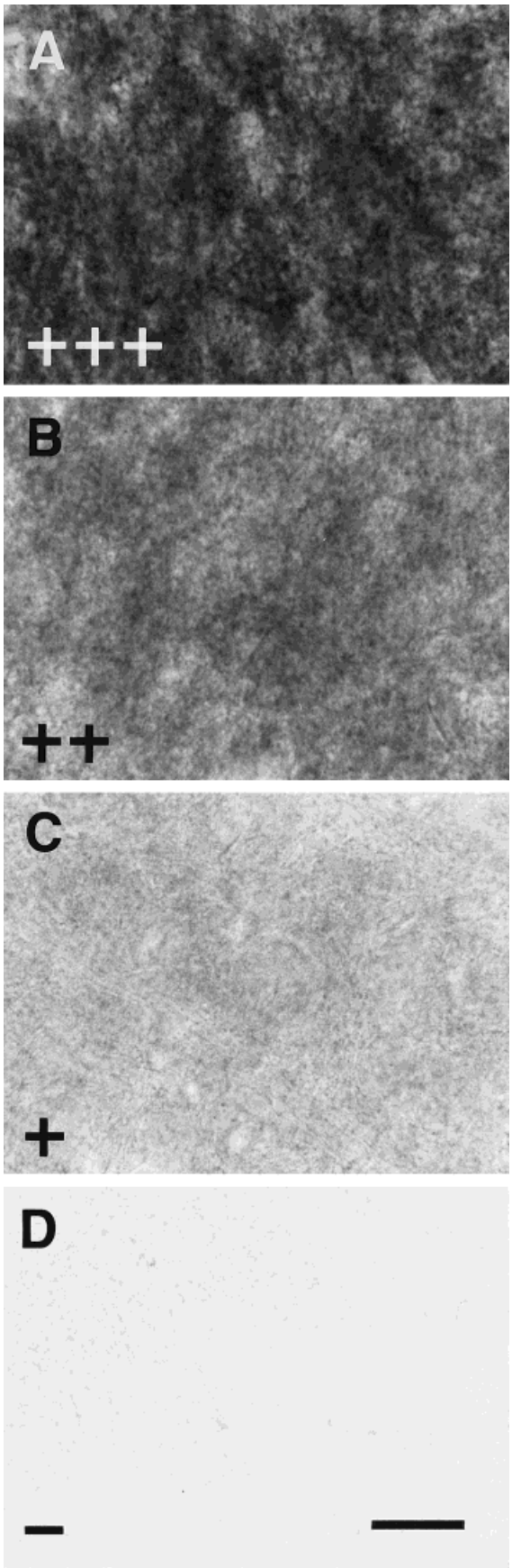

duncular nucleus. No neuronal cell bodies with EP3R-LI were observed in the basal ganglia or in the basal forebrain region.

In the lateral septal nucleus (Fig. 4A), neuronal cell bodies and fine processes with moderate or weak EP3R-LI were distributed sparsely in the intermediate and ventral parts (Fig. 8A), whereas no immunoreactivity was seen in the dorsal part. The septofimbrial nucleus also contained a few neuronal cell bodies with weak EP3R-LI (Fig. 4B). However, no EP3R-LI was detected in the medial septal nucleus or in the nucleus of the diagonal band.

Preoptic region and hypothalamus. Many neuronal cell bodies and fine processes with intense EP3R-LI were densely localized in the median preoptic nucleus and the medial preoptic area (Fig. 4A,B), as shown previously by Nakamura et al. (1999). The parastrial nucleus also contained a number of fine processes with intense EP3R-LI, but immunostained neuronal cell bodies were not detected in the nucleus. No EP3R-LI was observed in the lateral preoptic area, anteroventricular periventricular nucleus, or ventromedial preoptic nucleus.

EP3R-LI was intense in the neuropil of the compact part of the dorsomedial hypothalamic nucleus, as reported previously (Nakamura et al., 1999), and weak in the neuropil of the dorsal and ventral parts of the nucleus (Fig. 4F), although only the dorsal and ventral parts contained a few neuronal cell bodies with weak EP3R-LI. The immunostained neuropil of the dorsal and ventral parts of the dorsomedial hypothalamic nucleus seemed to spread over the perifornical and subincertal nuclei (Fig. 4F), in which scattered neuronal cell bodies exhibited moderate or weak EP3R-LI (Fig. 8B). Both of the periventricular and paraventricular hypothalamic nuclei showed moderate or weak EP3R-LI in the neuropil (Fig. 4D,E), whereas only the periventricular nucleus contained neuronal cell bodies with intense immunoreactivity (Fig. 8C). Weak EP3R-LI was observed in the neuropil of the anterior hypothalamic area (Fig. 4C), whereas neuronal cell bodies with moderate or weak EP3R-LI were scattered only in the posterior part of the area. The dorsal and posterior hypothalamic areas contained moderately or weakly immunostained neuronal cell bodies that were dispersed in the neuropil with weak EP3R-LI (Fig. 4G). However, EP3R-LI was not detected in the suprachiasmatic nucleus or the supraoptic nucleus.

In the mammillary body (Fig. 4H), intense or moderate EP3R-LI was observed in the neuropil of a region comprised of the median part of the medial mammillary nucleus, the dorsal part of the premammillary nucleus, and the ventral part of the supramammillary nucleus (Fig. 8D). Weak EP3R-LI was seen in the neuropil of the medial and lateral parts of the medial mammillary nucleus. However, no cell bodies showing EP3R-LI were distributed in those mammillary nuclei. Neuronal cell bodies with moderate or weak EP3R-LI were detected in the lateroposte-

Fig. 3. Internal standards for EP3R-like immunoreactivity (-LI). Intensity of EP3R-LI was ranked as follows: EP3R-LI was intense (+++) in neuropil of the paraventricular thalamic nucleus (**A**), moderate (++) in neuropil of the zonal and superficial gray layers of the superior colliculus (**B**), weak (+) in neuropil of the dorsal lateral geniculate nucleus (**C**), and negative (−) in neuropil of the paratenial thalamic nucleus (**D**). Scale bar = 20 μm.

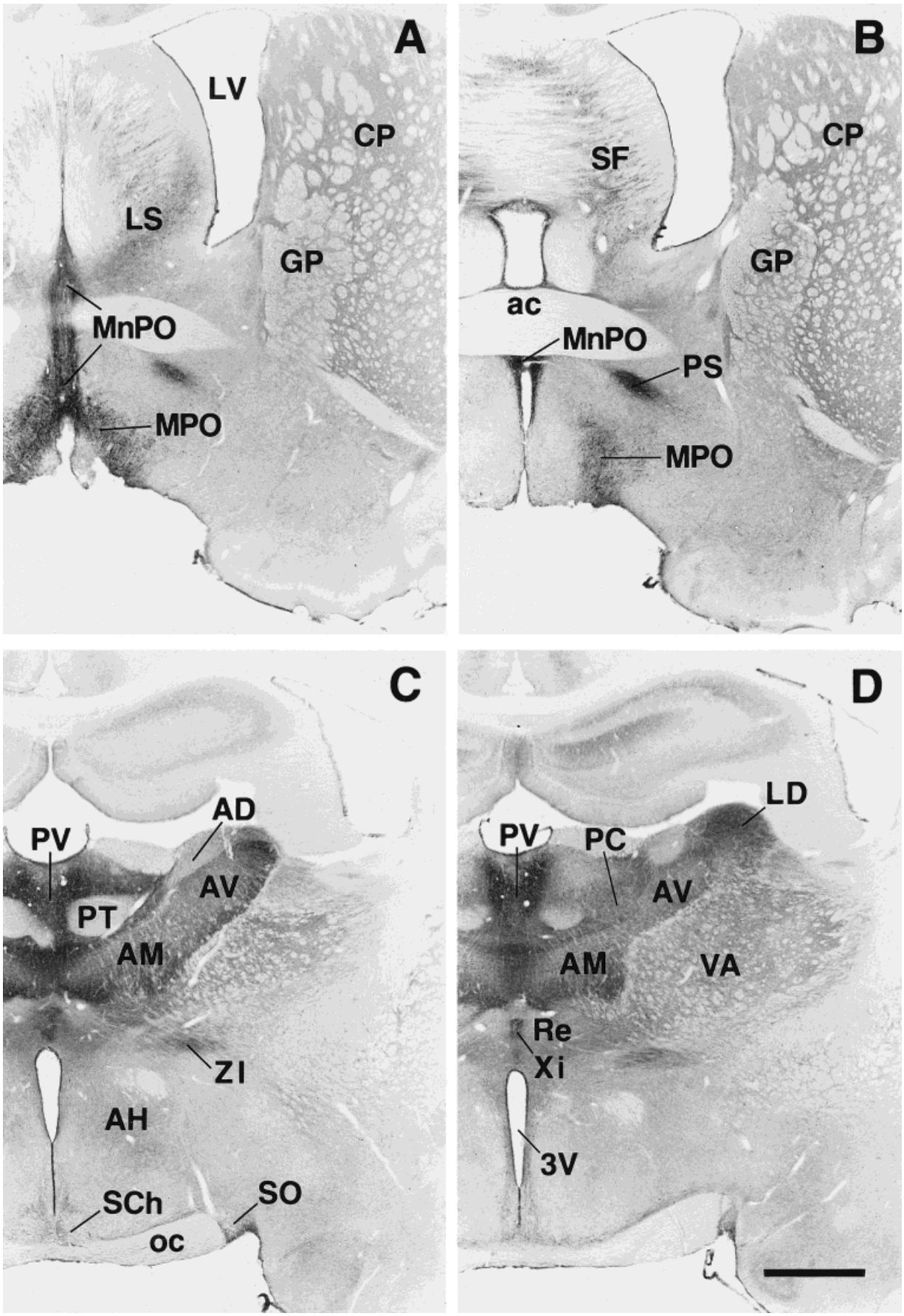

Fig. 4. **A–R:** Overview of EP3R-LI from the preoptic and septal regions to the medulla oblongata. Arrows indicate the fibers of the vagus nerve that exhibit EP3R-LI. For a detailed explanation, see text. For abbreviations, see list. Scale bar = 1 mm.

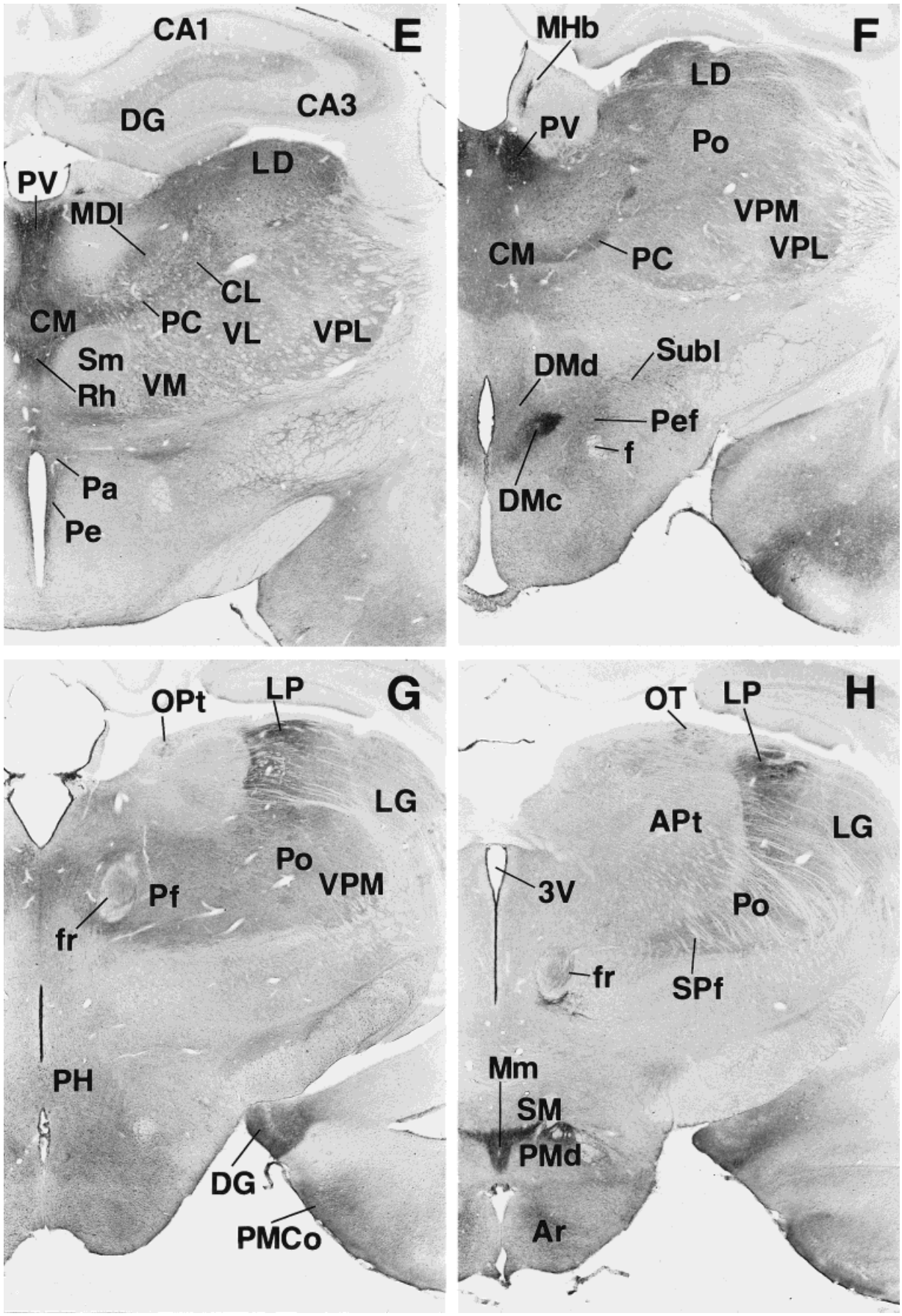

Figure 4 (Continued)

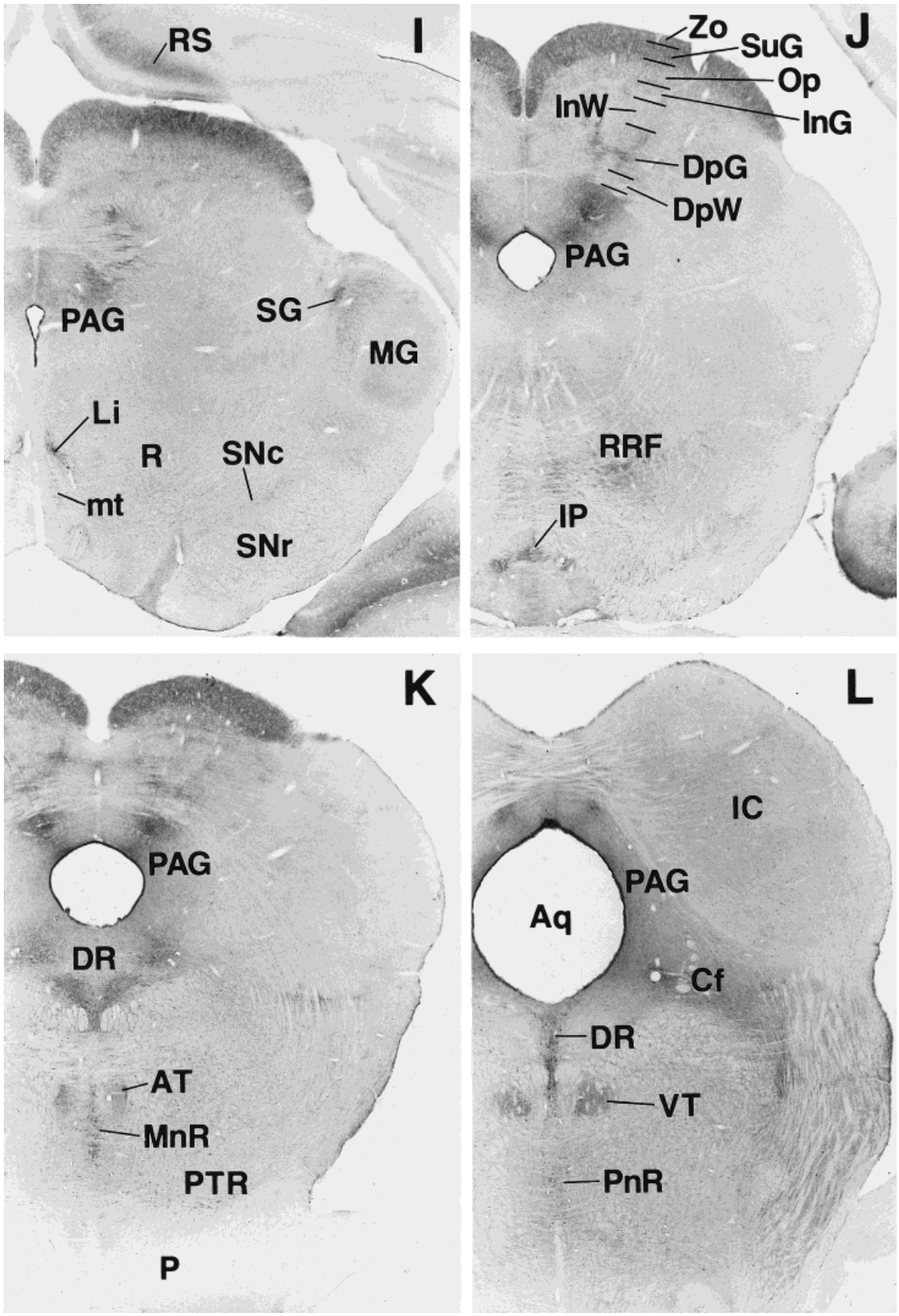

Figure 4 (Continued)

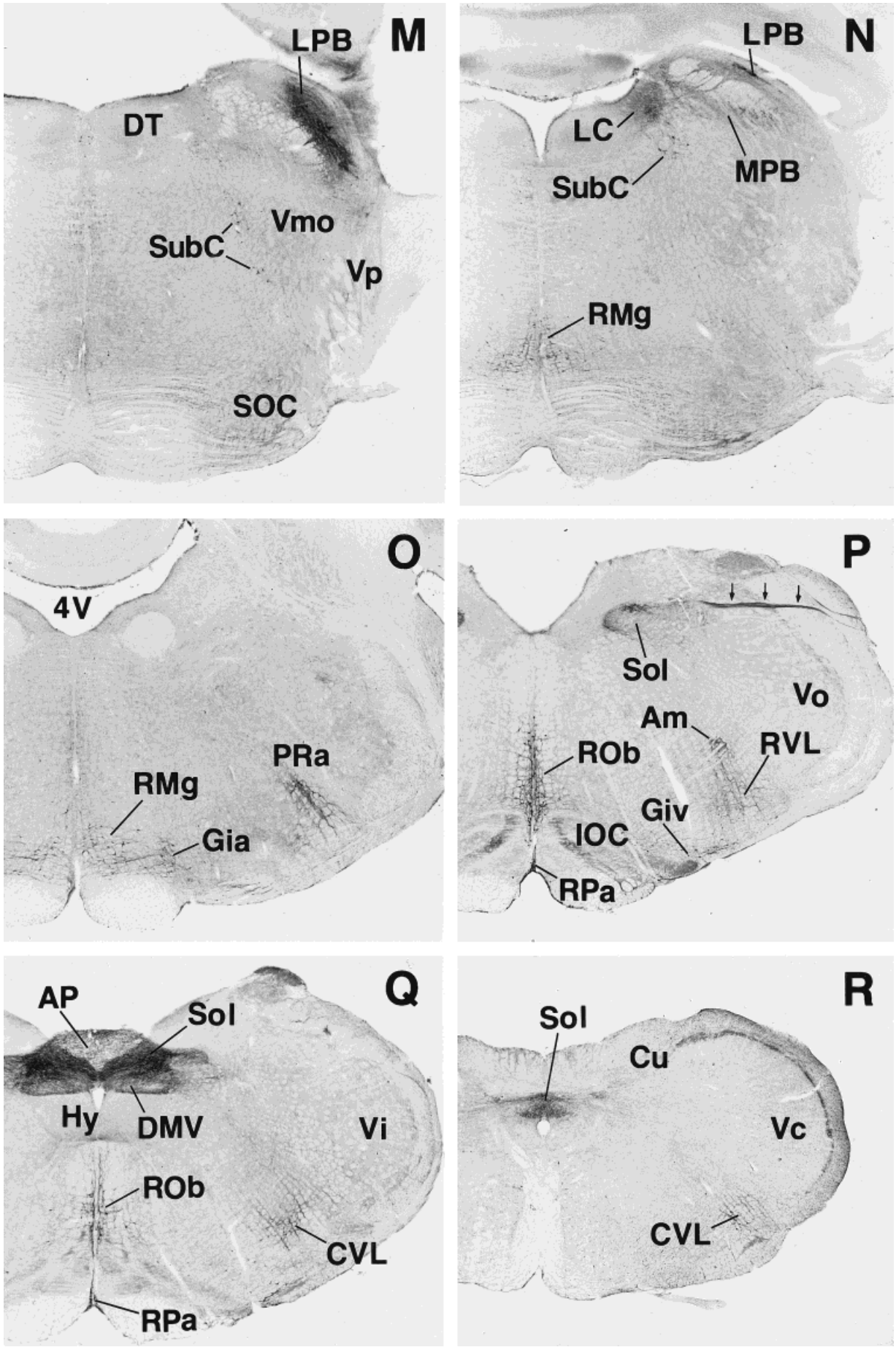

Figure 4 (Continued)

rior part of the arcuate nucleus, in which weak immunoreactivity also was detected in the neuropil.

Thalamus, epithalamus, and subthalamus. In the anterior nuclear group (Fig. 4C,D), EP3R-LI was intense or moderate in the neuropil of the anteroventral and anteromedial nuclei and moderate or weak in the neuropil of the anterodorsal nucleus. Granular EP3R-LI was detected in many neuronal cell bodies in the anteromedial nucleus (Fig. 9A), whereas no cell bodies with EP3R-LI were seen in the anteroventral or anterodorsal nuclei (Fig. 9B). In the mediodorsal nucleus (Fig. 4E), EP3R-LI was detected only in the lateral part, in which neuronal cell bodies with granular EP3R-LI were observed, and the neuropil also was immunostained weakly. The ventral nuclear complex (Fig. 4D–G) exhibited weak EP3R-LI in the neuropil, and neuronal cell bodies with weak EP3R-LI were distributed in the ventral anterior, ventral lateral, and ventral medial nuclei (Fig. 9C). However, no cell bodies with EP3R-LI were detected in the ventral posteromedial nucleus or the ventral posterolateral nucleus.

In the lateral nuclear group, the laterodorsal nucleus showed intense EP3R-LI in the neuropil of the rostral part (Fig. 4D) and moderate EP3R-LI in the neuropil of the caudal part (Fig. 4E,F), and many neuronal cell bodies with granular EP3R-LI were distributed throughout the rostrocaudal axis of the laterodorsal nucleus (Fig. 9D). The lateral posterior nucleus exhibited moderate or weak EP3R-LI in the neuropil (Fig. 4G,H). Although no cell bodies with EP3R-LI were observed in the mediocaudal part of the lateral posterior nucleus (Fig. 9E), moderate or weak immunoreactivity was detected in neuronal cell bodies in the other parts (Fig. 9F). The posterior nuclear group (Fig. 4F–H) contained many neuronal cell bodies with moderate or weak EP3R-LI and exhibited weak immunoreactivity in the neuropil.

Many neuronal cell bodies showing moderate or weak EP3R-LI were distributed throughout the intralaminar nuclear group (Fig. 9G). EP3R-LI was intense to moderate in the neuropil of the central medial and paracentral nuclei, moderate to weak in the neuropil of the central lateral nucleus (Fig. 4E,F), and weak in the neuropil of the parafascicular and subparafascicular nuclei (Fig. 4G,H). In the midline nuclear group (Fig. 4C–F), EP3R-LI was intense in the neuropil of the paraventricular, interanterodorsal, and interanteromedial nuclei and was moderate or weak in the neuropil of the intermediodorsal nucleus. Many neuronal cell bodies showing moderate EP3R-LI were distributed in the interanterodorsal, interanteromedial, and intermediodorsal nuclei, although the paraventricular nucleus contained no cell bodies with EP3R-LI (Fig. 3A). Intense or moderate EP3R-LI was observed in the neuropil of the xiphoid nucleus and of the caudal part of the rhomboid nucleus, and weak EP3R-LI was observed in the neuropil of the reuniens nucleus. Neuronal cell bodies showing intense or moderate EP3R-LI were densely packed in the caudal part of the rhomboid nucleus (Fig. 9H), and a few neuronal cell bodies with weak EP3R-LI were distributed in the reuniens and xiphoid nuclei. No EP3R-LI was detected in the paratenial nucleus (Fig. 3D), the rostral part of the rhomboid nucleus, or the submedius nucleus.

All parts of the lateral geniculate nucleus (Fig. 4G,H) showed weak-to-moderate immunoreactivity in the neuropil but did not contain any cell bodies with EP3R-LI (Fig. 3C). Neuronal cell bodies with weak or moderate EP3R-LI were localized in the suprageniculate and medial geniculate nuclei, which also exhibited weak EP3R-LI in the neuropil (Fig. 4I).

In the lateral part of the medial habenular nucleus, the neuropil and a few neuronal cell bodies with intense EP3R-LI were packed densely (Figs. 4F, 10A). However, no immunoreactivity was seen in the lateral habenular nucleus or in the medial part of the medial habenular nucleus. We detected weak EP3R-LI on the fibers of the fasciculus retroflexus (Fig. 4G,H) and also observed several neuronal cell bodies and fine dendritic processes exhibiting intense EP3R-LI by the side of the fasciculus retroflexus (Fig. 10B). In the zona incerta, the neuropil of the rostral part was immunostained moderately (Fig. 4C,D), but no immunoreactivity was detected in the intermediate or caudal parts.

Midbrain. Among the raphe nuclei belonging to the midbrain, the dorsal raphe nucleus contained many neuronal cell bodies and fine dendritic processes with moderate EP3R-LI (Figs. 4K,L, 13C). The median raphe nucleus also exhibited moderate or weak EP3R-LI in neuronal cells and a few fine processes (Figs. 4K, 13D). The rostral linear nucleus of the raphe contained a small number of intensely immunostained neuronal cell bodies and fine dendritic processes (Fig. 4I), whereas no EP3R-LI was seen in the caudal linear nucleus of the raphe.

In the dorsolateral part of the periaqueductal gray, the neuropil was immunostained moderately in the posterior two-thirds (Fig. 4J–L) and weakly in the anterior one-third (Fig. 4I). Several neuronal cell bodies with weak EP3R-LI were detected only in the anterior one-third of the dorsolateral part (Fig. 11A, arrows), but not in the posterior two-thirds (Fig. 11B). The other parts of the periaqueductal gray showed weak EP3R-LI in the neuropil of the caudal portion (Fig. 4K,L), although no immunoreactivity was detected in the rostral portion of the other parts of the periaqueductal gray.

EP3R-LI in the superior colliculus (Fig. 4I–K) was moderate in the neuropil of the zonal and superficial gray layers (Fig. 3B), moderate to weak in the neuropil of the deep gray layer, and weak in the neuropil of the optic nerve layer; whereas EP3R-LI was not seen in the intermediate gray layer, the intermediate white layer, or the deep white layer. In the pretectal area (Fig. 4G,H), EP3R-LI was weak in the neuropil of the olivary pretectal nucleus and the nucleus of the optic tract, although no immunoreactivity was seen in the anterior pretectal nucleus, medial pretectal nucleus, posterior pretectal nucleus, or precommissural nucleus. No neuronal cell bodies with EP3R-LI were found in the pretectal area or the superior colliculus.

Moderate or weak EP3R-LI was detected in the neuropil of the dorsomedial and dorsolateral subnuclei of the interpeduncular nucleus (Figs. 4J, 11C), whereas no immunoreactivity was seen in the other subnuclei of the nucleus. The retrorubral field (Fig. 4J) and the cuneiform nucleus (Figs. 4L, 11D) also showed moderate or weak EP3R-LI in the neuropil, and the anterior and ventral tegmental nuclei exhibited weak immunoreactivity in the neuropil (Fig. 4K,L). However, neuronal cell bodies with EP3R-LI were not seen in the interpeduncular nucleus, cuneiform nucleus, retrorubral field, or anterior or ventral tegmental nuclei. On the mammillotegmental tract, we could also observe weak EP3R-LI (Fig. 4I). No EP3R-LI was detected in the

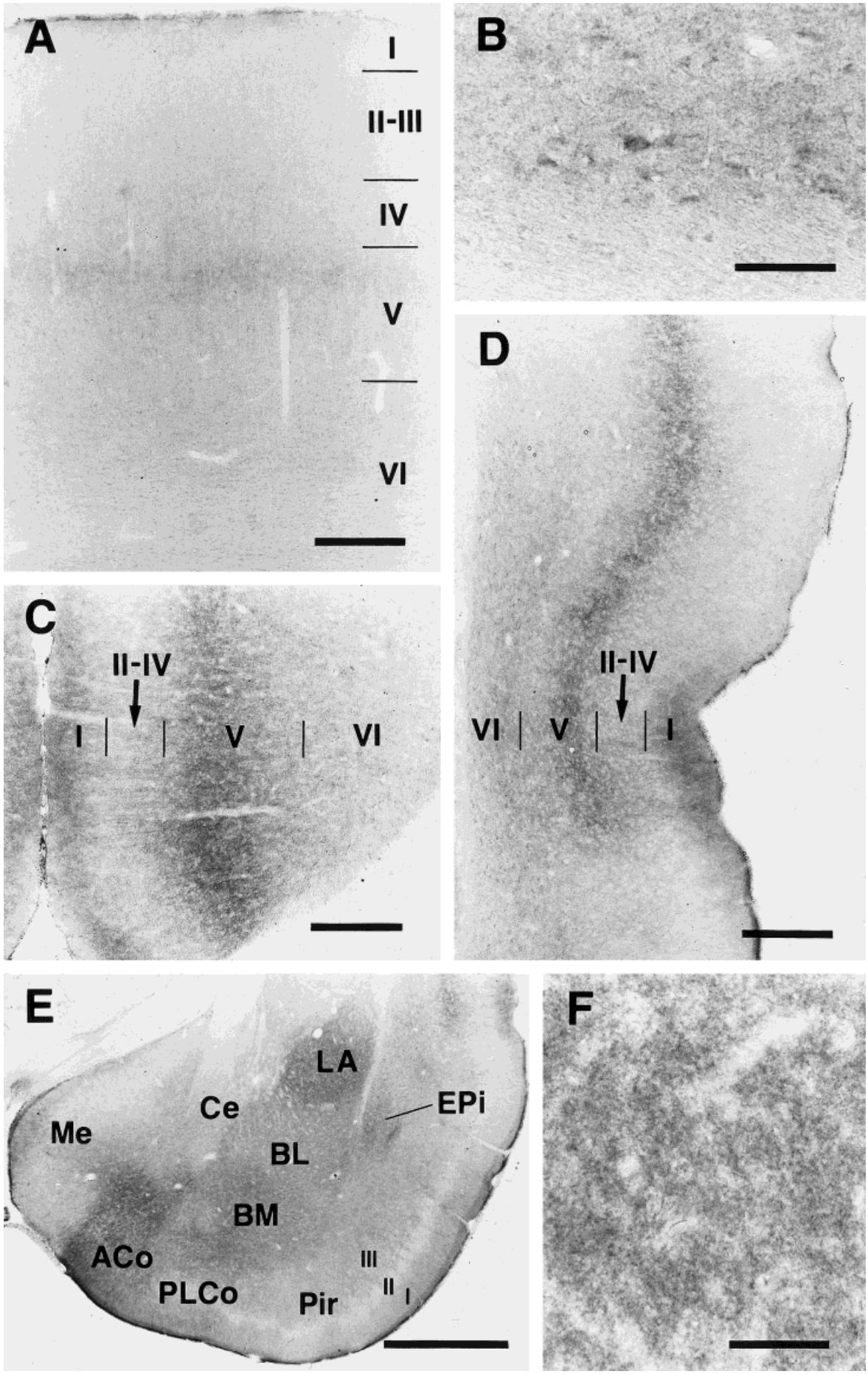
A
I
II-III
IV
V
VI
B
C
II-IV
I
V
VI
D
II-IV
VI
V
I
E
LA
Ce
EPi
Me
BL
BM
ACo
III
II
I
PLCo
Pir
F

Figure 5

Edinger-Westphal nucleus, oculomotor or trochlear nuclei, terminal nuclei of the accessory optic tract, substantia nigra, ventral tegmental area, red nucleus, inferior colliculus, or mesencephalic trigeminal nucleus.

Pons. In the lateral parabrachial nucleus (Fig. 4M,N), EP3R-LI was intense to moderate in the neuropil of the external, central, and crescent parts and moderate in the neuropil of the dorsal part, although no EP3R-LI was shown in the ventral or internal parts. Cell bodies with EP3R-LI could not be detected in the lateral parabrachial nucleus (Fig. 11E). Some neuronal groups comprised of small cells exhibited intense EP3R-LI in the caudal part of the medial parabrachial nucleus (Figs. 4N, 11F), in which weak EP3R-LI also was observed in the neuropil, whereas no immunoreactivity was seen in the rostral part of the medial parabrachial nucleus.

Many dendritic processes were immunostained moderately in the locus coeruleus (Fig. 4N), although the numbers of neuronal cell bodies exhibiting EP3R-LI were small (Fig. 13A, arrow). In the subcoeruleus nucleus, we detected scattered neuronal cell bodies showing intense EP3R-LI (Figs. 4M, 13B). This positive cell group in the subcoeruleus nucleus extended in a dorsocaudal direction and finally fused with the locus coeruleus (Fig. 4N).

Neuronal cell bodies exhibiting intense EP3R-LI were scattered in the pontine tegmental reticular nucleus (Figs. 4K, 13F). In the pontine raphe nucleus, some neuronal cell bodies showed moderate or weak EP3R-LI, and weak immunoreactivity also was detected in the neuropil (Fig. 4L). We observed scattered neuronal cell bodies and fine processes showing intense EP3R-LI in the ventral portion of the alpha part of the parvicellular reticular nucleus (Figs. 4O, 11G). No EP3R-LI was seen in the dorsal tegmental nucleus, superior olivary complex, nucleus of the trapezoid body, motor trigeminal nucleus, principal sensory trigeminal nucleus, or pontine nuclei.

Medulla oblongata. In the nucleus of the solitary tract (Fig. 4P–R), EP3R-LI was intense in the neuropil of the commissural part (Fig. 12A), intense to moderate in the neuropil of the medial and intermediate parts, and weak in the neuropil of the ventrolateral part. In the rostral half of the nucleus, the medial (Fig. 12B) and intermediate parts (Fig. 12C) contained nerve fibers with intense or moderate EP3R-LI. The intermediate part also possessed intense and granular immunosignals forming a soma-like shape (Fig. 12C). We could not judge whether the immunoreactive structures with the soma-like shape were neuronal cell bodies with EP3R-LI, because it was possible that axon terminals with EP3R-LI surrounded immunonegative neuronal cell bodies. Intense EP3R-LI also was observed in many axons of the vagus nerve (Fig. 4P, arrows; Fig. 12D).

In the dorsal motor nucleus of the vagus nerve (Fig. 4Q), moderate EP3R-LI was seen in the neuropil, and several neuronal cell bodies showing weak EP3R-LI were detected especially in the medial portion (Fig. 14A). The ambiguus nucleus exhibited moderate EP3R-LI in the neuropil of the rostral part (Figs. 4P, 14B), although the caudal part showed no immunoreactivity. In an area immediately ventral to the ambiguus nucleus, which belongs to the rostroventrolateral or caudoventrolateral reticular nucleus and was referred to as the external formation of the ambiguus nucleus in a previous study (Bieger and Hopkins, 1987), we observed scattered neuronal cell bodies and fine processes with intense or moderate EP3R-LI (Fig. 4P–R; Fig. 14B, arrows). Because signals in the area postrema had barely disappeared by preincubation of the primary antibody with the immunogen, we could not evaluate EP3R-LI in the region.

Neuronal cell bodies and fine dendritic processes exhibiting intense EP3R-LI were distributed in the raphe magnus, raphe obscurus, and raphe pallidus nuclei (Figs. 4N–Q, 13E). The positive neuronal group in these raphe nuclei extended into the lateral portions of the alpha and ventral parts of the gigantocellular reticular nucleus (Fig. 4O,P). In the caudal part of the spinal trigeminal nucleus, only laminae I and II exhibited EP3R-LI in the neuropil (Fig. 4R). The EP3R-LI was intense to moderate in lamina II and weak in lamina I (Fig. 11H). Weak EP3R-LI was detected in the neuropil of the medial part of the principal nucleus of the inferior olivary complex (Fig. 4P), although other parts of the inferior olivary complex did not exhibit EP3R-LI. No EP3R-LI was seen in the cochlear nuclei, abducens nucleus, facial nucleus, vestibular nuclei, hypoglossal nucleus, external cuneate and cuneate nuclei, gracile nucleus, prepositus hypoglossal nucleus, or lateral reticular nucleus.

Spinal cord and peripheral ganglia. In all of the spinal segments (Fig. 6A–F), the neuropil of lamina II and lamina I showed moderate and weak EP3R-LI, respectively (Fig. 6G). In some sequential sections from each spinal segment, intense EP3R-LI was detected in the neuropil of the inner zone of lamina II. Neither laminae contained any neuronal cell bodies with EP3R-LI. The intermediolateral nucleus of the cervicothoracic cord showed moderate EP3R-LI in the neuropil and contained a few neuronal cell bodies with weak immunoreactivity (Figs. 6B,C, 14C). Several neuronal cell bodies and fine processes exhibited moderate EP3R-LI in the sacral parasympathetic nucleus (Figs. 6E, 14D).

In the trigeminal and dorsal root ganglia (Fig. 7), many neuronal cell bodies showed EP3R-LI. Most of the positive cells exhibited moderate or weak EP3R-LI and appeared to be classified as small neurons, whereas a small number of large or medium-sized positive cells showed intense immunoreactivity. The nodose ganglion also contained many neuronal cell bodies with intense or moderate EP3R-LI (Fig. 12E). In those sensory ganglia, EP3R-LI was found on the surface membrane of the neuronal cell bodies, and granular immunosignals were observed frequently in the cytoplasm. Axons with EP3R-LI also were detected in those ganglia, and some were continuous with immunostained cell bodies (Fig. 7A, arrows). In the sympathetic ganglia, a small number of the superior cervical and stellate ganglion cells exhibited EP3R-LI (data not shown).

Fig. 5. EP3R-LI in the cerebral cortex and amygdala. **A:** Primary somatosensory cortex. **B:** Neuronal cell bodies with EP3R-LI in layer VI of the primary somatosensory cortex. **C:** Cingulate cortex. **D:** Perirhinal and ectorhinal cortices. **E:** Amygdaloid body, piriform cortex, and endopiriform nucleus. **F:** Immunostained neuropil in the lateral amygdaloid nucleus. For abbreviations, see list. Scale bars = 300 μm in A,C,D; 50 μm in B,F; 1 mm in E.

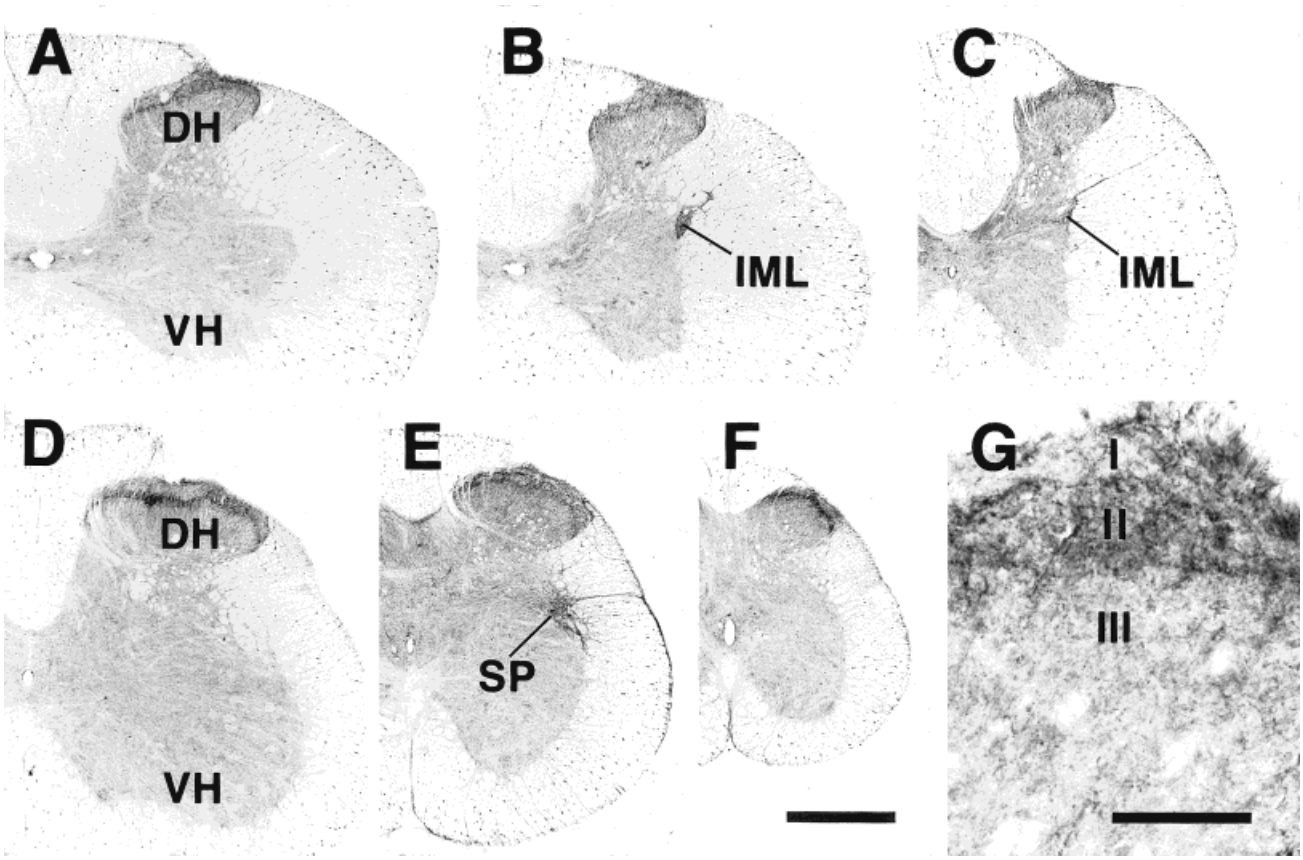

Fig. 6. Distribution of EP3R-LI in the spinal cord. **A:** Middle cervical segment. **B:** Lower cervical segment. **C:** Middle thoracic segment. **D:** Middle lumbar segment. **E:** Upper sacral segment. **F:** Lower sacral segment. **G:** Immunostained neuropil in superficial laminae of the dorsal horn in a cervical segment. Signals seen in the white matter were not absorbed by preincubation of the primary antibody with an excess amount of the antigen. For abbreviations, see list. Scale bars = 500 μm in F (also applies to A–E); 100 μm in G.

DISCUSSION

Glycosylated EP3R protein

In the immunoblotting analysis, the antibody specific to rat EP3R exhibited several immunoreactive bands with different molecular weights in immunopurified protein from rat brains and in membrane protein of rat EP3β receptor-expressing COS-7 cells. After deglycosylation, most of those immunoreactive bands came to show an apparently single entity with a molecular weight of ≈ 33 kDa. This result indicates that EP3R protein molecules are modified posttranslationally with different sizes of carbohydrate moieties, and, thereby, several forms of glycoproteins are produced. In a recent study, mutations at two deduced *N*-glycosylation sites of mouse EP3α receptor affected the affinity and specificity of the ligand binding (Huang and Tai, 1998). Therefore, the various types of carbohydrate moieties may have some modulatory roles in the physiologic functions of EP3R.

To obtain further detailed information on EP3R protein, the deglycosylated receptor protein was analyzed with electrophoresis in a urea-containing polyacrylamide gel, which could well separate proteins at around 30 kDa. Two adjacent immunoreactive bands were detected in the lane of the brain, whereas only a single band was seen in the lane of the COS-7 cells. Because rat EP3R has three isoforms with similar molecular weights deduced from their amino-acid sequences, 39.9 kDa (EP3α), 39.6 kDa (EP3β), and 39.5 kDa (EP3γ; Takeuchi et al., 1993, 1994; Kitanaka et al., 1996), it is likely that the two bands were derived from the isoforms endogenously expressed in the rat brain. On the other hand, the single band may be formed by EP3β isoform expressed in the culture cells. Moreover, the two immunoreactive bands in the brain showed higher molecular weights than the single band in the COS-7 cells. This may arise from protein modifications specific in the brain, such as the addition of phosphate groups on the protein, as seen in other receptors (Ji et al., 1998).

Correlations between EP3R distribution and functions

The distribution of EP3R-LI observed in this study was highly similar to that of PGE_2 binding sites identified by quantitative autoradiography using radiolabelled PGE_2 (Matsumura et al., 1990, 1992). This fact enhances the reliability of our immunohistochemical investigation and suggests that the current results show the distribution of functional EP3R. Furthermore, the high similarity indicates that many of the CNS actions of PGE_2 may be ascribable to EP3R among the four PGE receptor subtypes.

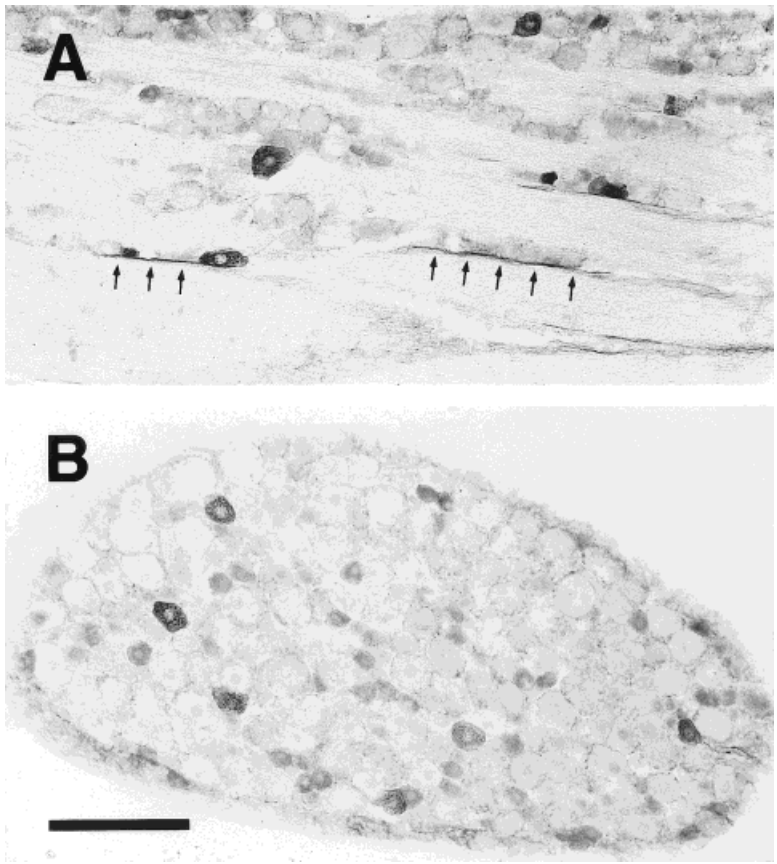

Fig. 7. EP3R-LI in the trigeminal ganglion (**A**) and the dorsal root ganglion (**B**). Arrows indicate the axons that show EP3R-LI. Scale bar = 200 μm.

We observed neuronal cell bodies exhibiting EP3R-LI in several monoamine-containing nuclei. Among them, the locus coeruleus and subcoeruleus nucleus contain A6 and A7 noradrenaline cell groups, respectively. In the locus coeruleus, EP3R appears to be located on somatodendritic plasma membrane, because many fine processes and a few neuronal cell bodies with EP3R-LI were densely localized, and a previous in situ hybridization study showed intense signals for mouse EP3R mRNA in the nucleus (Sugimoto et al., 1994). Because the locus coeruleus, through its massively divergent efferent projections, has been implicated in vigilance, alertness, orientation, and attention (for reviews, see Aston-Jones et al., 1991; Foote et al., 1991), EP3R may play a role in these attentional processes by regulating the inputs to the nucleus postsynaptically. In addition to the noradrenergic cell groups, neuronal cells with EP3R-LI were seen in most of the raphe nuclei, which contain serotonergic cell groups. Furthermore, scattered neuronal cell bodies showing EP3R-LI also were detected in the pontine tegmental reticular nucleus, where the B9 serotonin cell group is found. The distribution patterns of the neuronal cells with EP3R-LI in the nuclei are quite similar to the immunostaining patterns seen with anti-serotonin antibodies (Steinbusch, 1981; Törk, 1985). An electrophysiologic study showed previously that direct agonist activation of EP3R led to excitation of putative serotonergic neurons in the rat dorsal raphe nucleus (Momiyama et al., 1996). Therefore, it is possible that EP3R, when it is placed on the postsynaptic membrane of serotonin-containing neurons, modulates the activities of the neurons and, thus, affects the physiologic actions of the serotonin system, such as analgesia mediated by serotonergic neurons descending from the raphe magnus nucleus to the spinal cord (Mohrland and Gebhart, 1980; Vasko et al., 1984). In light of our previous observation of signals for EP3R mRNA in the compact part of the substantia nigra (Sugimoto et al., 1994), in which many dopamine-containing neurons are localized, dopaminergic neurons also may express EP3R. However, we could not detect EP3R-LI in the substantia nigra or the ventral tegmental area. In the caudate-putamen, one of the major dopaminergic projection sites from those regions, weak EP3R-LI was found. Thus, a small amount of EP3R protein possibly may be located on axon terminals projected from the dopaminergic neurons residing in the substantia nigra.

EP3R-LI was observed in some of the nuclei controlling the autonomic nervous system. In the medulla oblongata, neuronal cells with EP3R-LI were observed in the dorsal motor nucleus of the vagus nerve, which contains preganglionic neurons of the parasympathetic nervous system. Moreover, some neuronal cells and fine dendritic processes showing intense EP3R-LI were found in the external formation of the ambiguus nucleus, which was shown

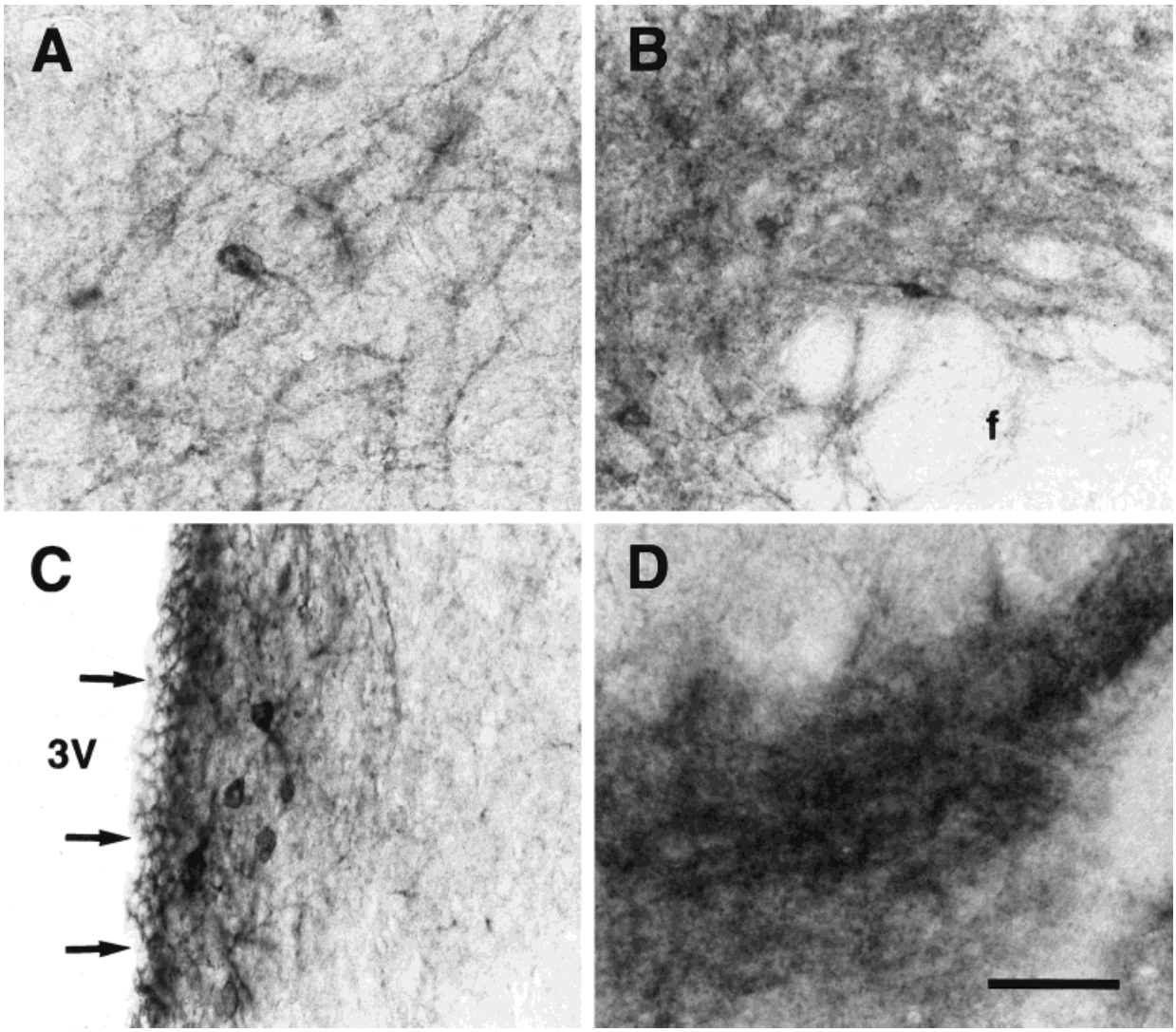

Fig. 8. EP3R-LI in the intermediate part of the lateral septal nucleus (**A**), the perifornical nucleus (**B**), the periventricular hypothalamic nucleus (**C**), and the dorsal part of the premammillary nucleus (**D**). Arrows indicate the ependymal layer exhibiting EP3R-LI. 3V, third ventricle; f, fornix. Scale bar = 50 μm.

previously to contain parasympathetic preganglionic neurons innervating the heart and supradiaphragmatic structures (Bieger and Hopkins, 1987). At the sacral cord level, the parasympathetic preganglionic neurons also appeared to exhibit EP3R-LI. We could not identify the expression of EP3R in the other parasympathetic nuclei, including the salivatory nuclei and the Edinger-Westphal nucleus. In the sympathetic nervous system, preganglionic neurons are located in the intermediolateral nucleus of lower cervical and all thoracic segments. EP3R-LI was observed in the neuropil and in several neuronal cell bodies of the intermediolateral nucleus, suggesting that a population of the sympathetic preganglionic neurons express EP3R. These results indicate that EP3R may regulate the output mediated by those autonomic preganglionic neurons from the CNS. However, most of pharmacologic studies on the functions of PGE_2 in the autonomic nervous system have focused thus far on the EP3R that is located on peripheral terminals of the autonomic postganglionic nerve fibers (Mantelli et al., 1991; Molderings et al., 1992, 1994; Reinheimer et al., 1998; Spicuzza et al., 1998). Therefore, the distribution of EP3R-LI in this study may help to reveal the unknown roles of PGE_2 in the central autonomic system.

The nucleus of the solitary tract showed intense EP3R-LI in the neuropil. Because EP3R-LI also was seen

Fig. 9. EP3R-LI in the thalamus. **A:** Anteromedial nucleus. **B:** Anteroventral nucleus. **C:** Ventral medial nucleus. **D:** Laterodorsal nucleus. **E:** Mediocaudal part of the lateral posterior nucleus. **F:** Mediorostral part of the lateral posterior nucleus. **G:** Central lateral nucleus. **H:** Reuniens nucleus. Scale bar = 50 μm.

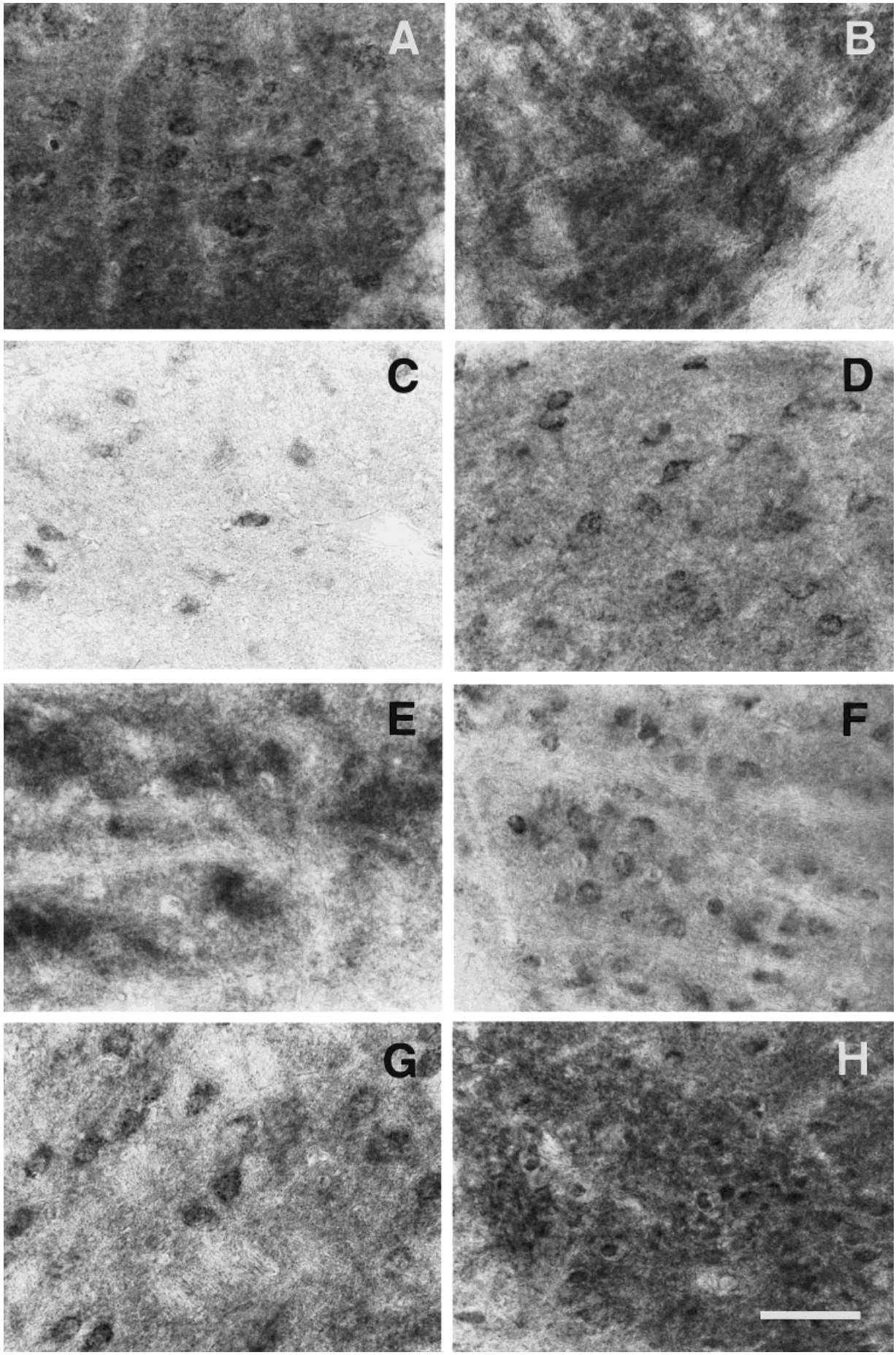

Figure 9

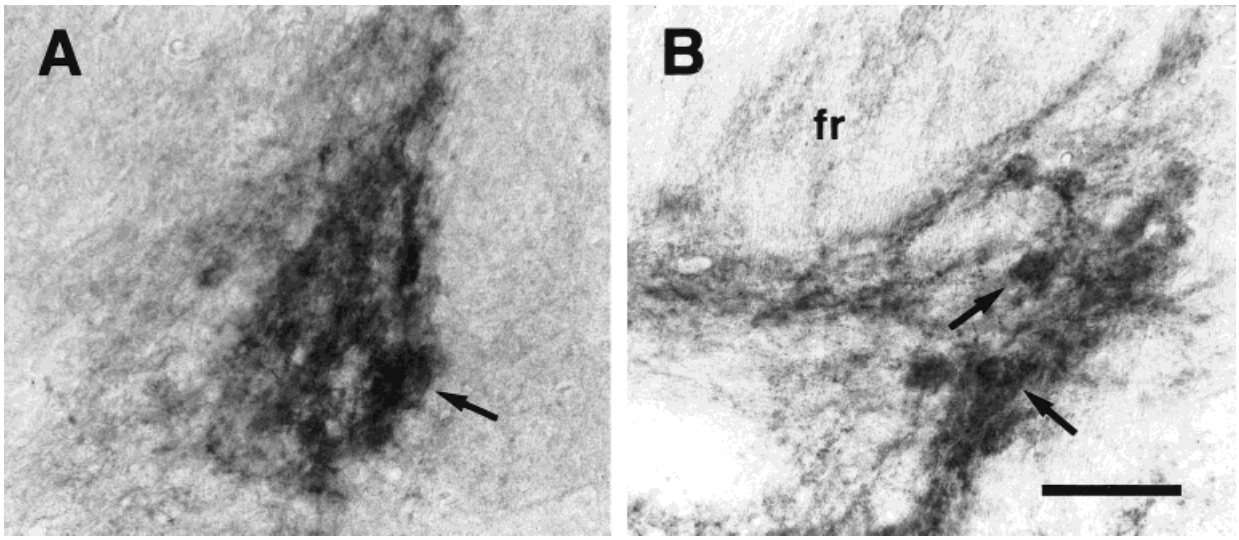

Fig. 10. EP3R-LI in the medial habenular nucleus (**A**) and the fasciculus retroflexus (**B**). Neuronal cell bodies with intense EP3R-LI (A, arrow) were distributed sparsely in the lateral part of the medial habenular nucleus. Arrows in B indicate the neuronal cells exhibiting EP3R-LI located by the side of the fasciculus retroflexus (fr). Scale bar = 50 μm.

in the nodose ganglion and axons of the vagus nerve, it seems reasonable to suppose that EP3R is distributed on the central endings of the vagus nerve and that the presynaptic EP3R in the nucleus of the solitary tract modulates inflow of visceral sensory information through the vagus nerve. Other researchers recently showed that mRNAs for EP3R and interleukin-1 receptor were expressed within the rat nodose ganglion and that an increase in the discharge activity of gastric vagal afferents after administration of interleukin-1β was attenuated by pretreatment with indomethacin, an inhibitor of PG synthesis, suggesting that PG is necessary for part of the cytokine-induced activation of vagal sensory functions (Ek et al., 1998). Because activation of the vagal sensory system is thought to be necessary for the CNS response during local infections in the abdominal or thoracic cavities (Elmquist et al., 1997), it is likely that PGE_2 plays an essential role in the immune response of the CNS through EP3R in the vagal afferent system. Lately, one of the other PGE receptor subtypes, EP4, was shown to be expressed in neurons of the nucleus of the solitary tract by in situ hybridization (Zhang and Rivest, 1999). Although it has not yet been clarified whether EP4 receptor protein is located in the nucleus or in the projection sites, PGE_2 may exert dual modulatory functions in the transmission of visceral sensory information through the two different receptor subtypes.

It has been reported that intrathecal administration of PGE_2 into mice induced hyperalgesic effects to noxious stimuli (Taiwo and Levine, 1988; Uda et al., 1990), and a part of this PGE_2 action has been supposed to involve EP3R (Minami et al., 1994). However, the neuronal mechanism for the EP3R-mediated hyperalgesia remains obscure. The dorsal horn of the spinal cord is an important site for pain transmission, and we observed EP3R-LI in the neuropil of laminae I and II of the spinal dorsal horn throughout the full length of the spinal cord. This result is consistent with a recent study that examined only the lumbar spinal segments (Beiche et al., 1998). Furthermore, EP3R-LI also was observed in the dorsal root ganglia of all spinal segments, where both small and large neurons exhibited immunoreactivity, and the small neurons were the majority. This neuronal population seems to be in agreement with the distribution of EP3R mRNA in the mouse dorsal root ganglion (Sugimoto et al., 1994). Sensory neurons in the dorsal root ganglion terminate in laminae I and II of the spinal cord. There is sufficient evidence to show that the EP3R-LI observed in the dorsal horn is derived from the EP3R-expressing sensory neurons in the dorsal root ganglion. We have found that the intensity of the EP3R-LI in the dorsal horn was reduced substantially by unilateral dorsal rhizotomy (Yun-Qing Li, K.N., M.N., T.K., personal communication). Consonant with our observation, it was reported that unilateral dorsal rhizotomy decreased the density of tritiated PGE_2 binding sites in the dorsal horn (Matsumura et al., 1995). Thus, EP3R most likely is located on the central endings of the primary afferent fibers of the sensory neurons, and it may modulate pain transmission and may be involved in PGE_2-induced hyperalgesia.

The distribution pattern of EP3R-LI also implied the receptor's modulatory functions in the visual system. Immunoreactivity was detected in the neuropil of the lateral geniculate nucleus, olivary pretectal nucleus, nucleus of the optic tract, superficial gray and optic nerve layers of the superior

Fig. 11. EP3R-LI in the anterior (**A**) and posterior (**B**) portions of the periaqueductal gray, the interpeduncular nucleus (**C**), the cuneiform nucleus (**D**), the lateral parabrachial nucleus (**E**), the medial parabrachial nucleus (**F**), the alpha part of the parvicellular reticular nucleus (**G**), and the superficial laminae of the caudal part of the spinal trigeminal nucleus (**H**). In the periaqueductal gray, neuronal cells with EP3R-LI (A, arrows) were observed in the anterior part, whereas the posterior part showed EP3R-LI only in neuropil (B). Scale bar = 50 μm.

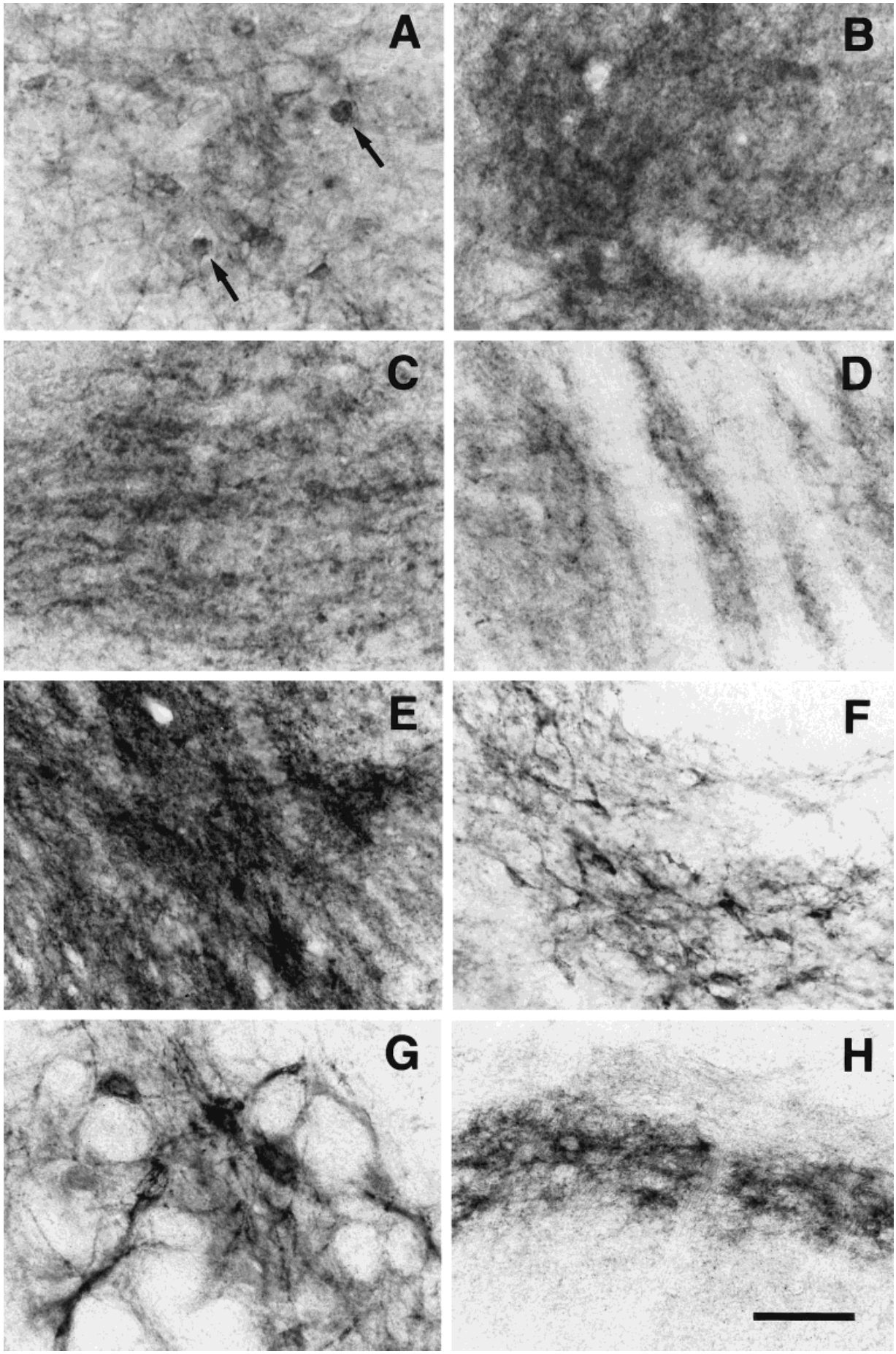

Figure 11

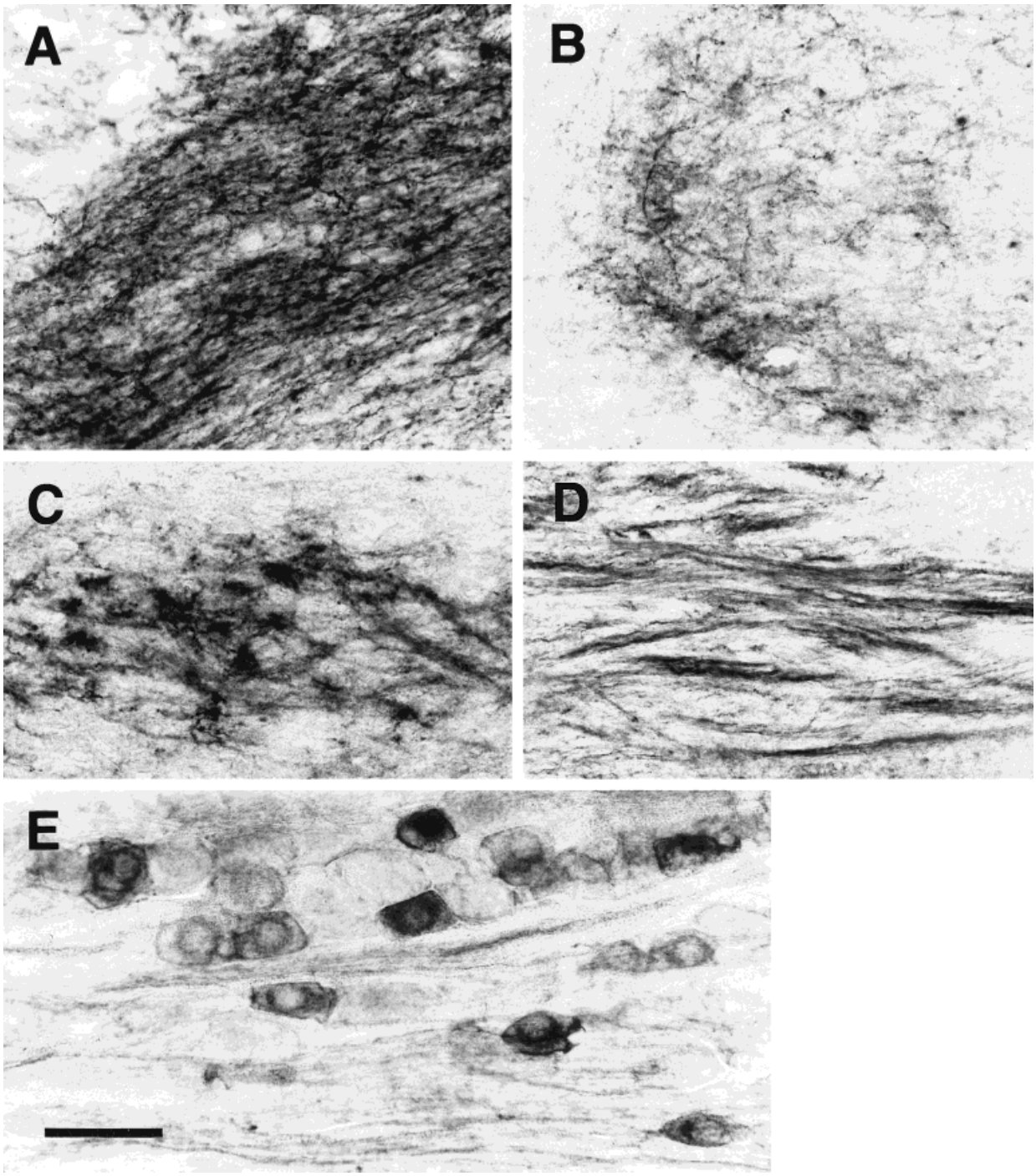

Fig. 12. EP3R-LI in the vagal pathway. In the nucleus of the solitary tract, EP3R-LI was observed in the commissural (**A**), medial (**B**), and intermediate (**C**) parts. EP3R-LI also was seen in the solitary tract (**D**) and the nodose ganglion (**E**). Scale bar = 50 μm.

colliculus, and lateral posterior thalamic nucleus, all of which are known to be innervated by retinal axons (for review, see Sefton and Dreher, 1995). In another line of evidence, an immunohistochemical report on porcine ocular tissues showed expression of EP3α receptor in ganglion cells of the retina (Zhao and Shichi, 1995). However, we could not find any immunoreactivity in the suprachiasmatic nucleus or terminal nuclei of the accessory optic tract, which also are retinorecipient nuclei, suggesting that a population of retinal ganglion cells does not express EP3R. In addition to vision, olfaction also may be modulated by EP3R. Although the olfactory bulb showed no EP3R-LI, mouse EP3R mRNA has

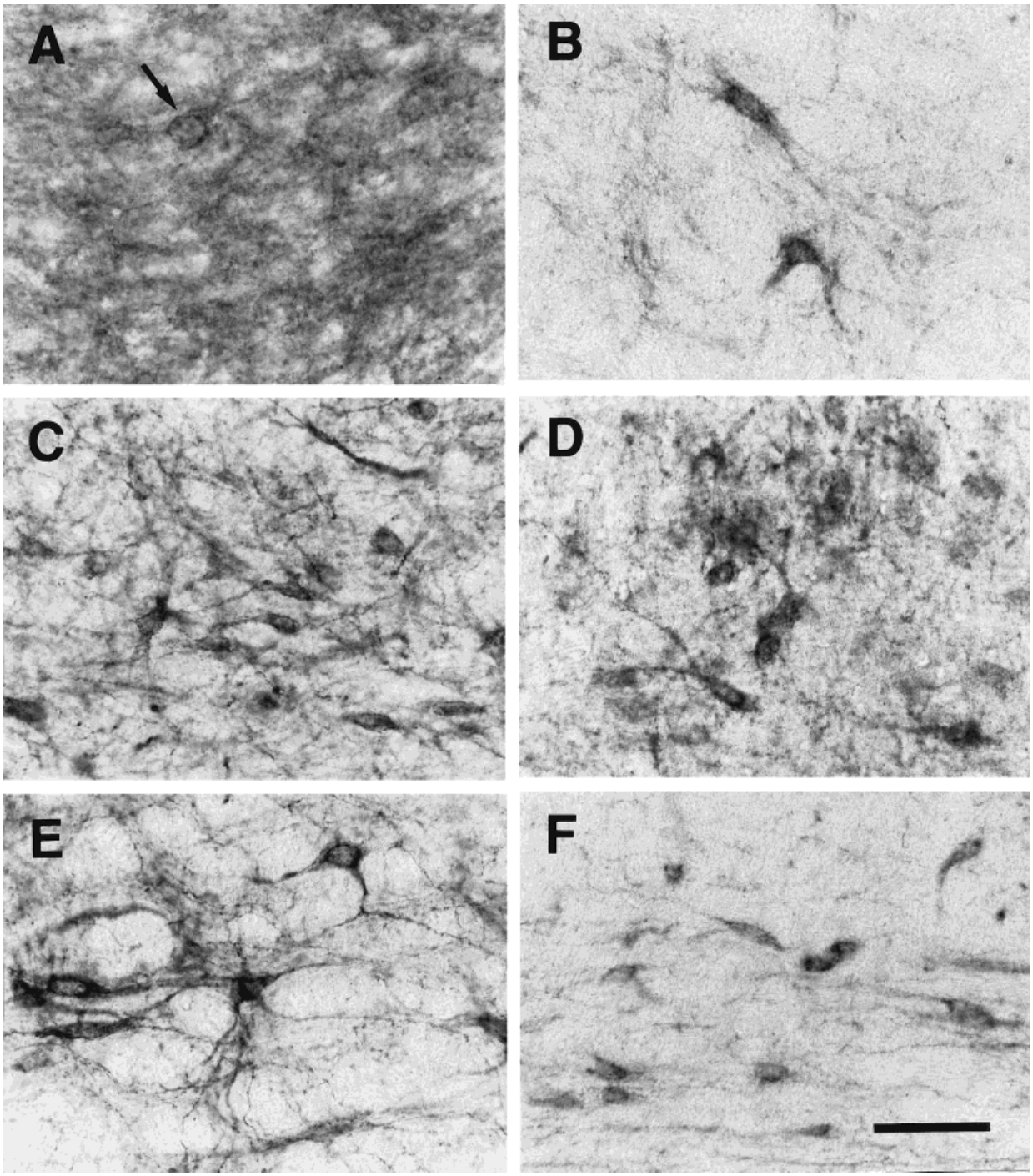

Fig. 13. EP3R-LI in the monoamine-containing nuclei. **A:** Locus coeruleus. Neuronal cell bodies with EP3R-LI (arrow) were distributed sparsely. **B:** Subcoeruleus nucleus. **C:** Dorsal raphe nucleus. **D:** Median raphe nucleus. **E:** Raphe magnus nucleus. **F:** Pontine tegmental reticular nucleus. Scale bar = 50 μm.

been shown to be expressed in mitral cells of the main and accessory olfactory bulbs (Sugimoto et al., 1994). Moreover, EP3R-LI was detected in the neuropil of layer I of the piriform cortex, the superficial part of which receives most of the afferent fibers from the mitral cells directly. These results indicate that, in the visual and olfactory systems, the EP3R located on the central terminals of the sensory fibers may play some regulatory roles in the synaptic transmission conveying sensory information to the central processing system.

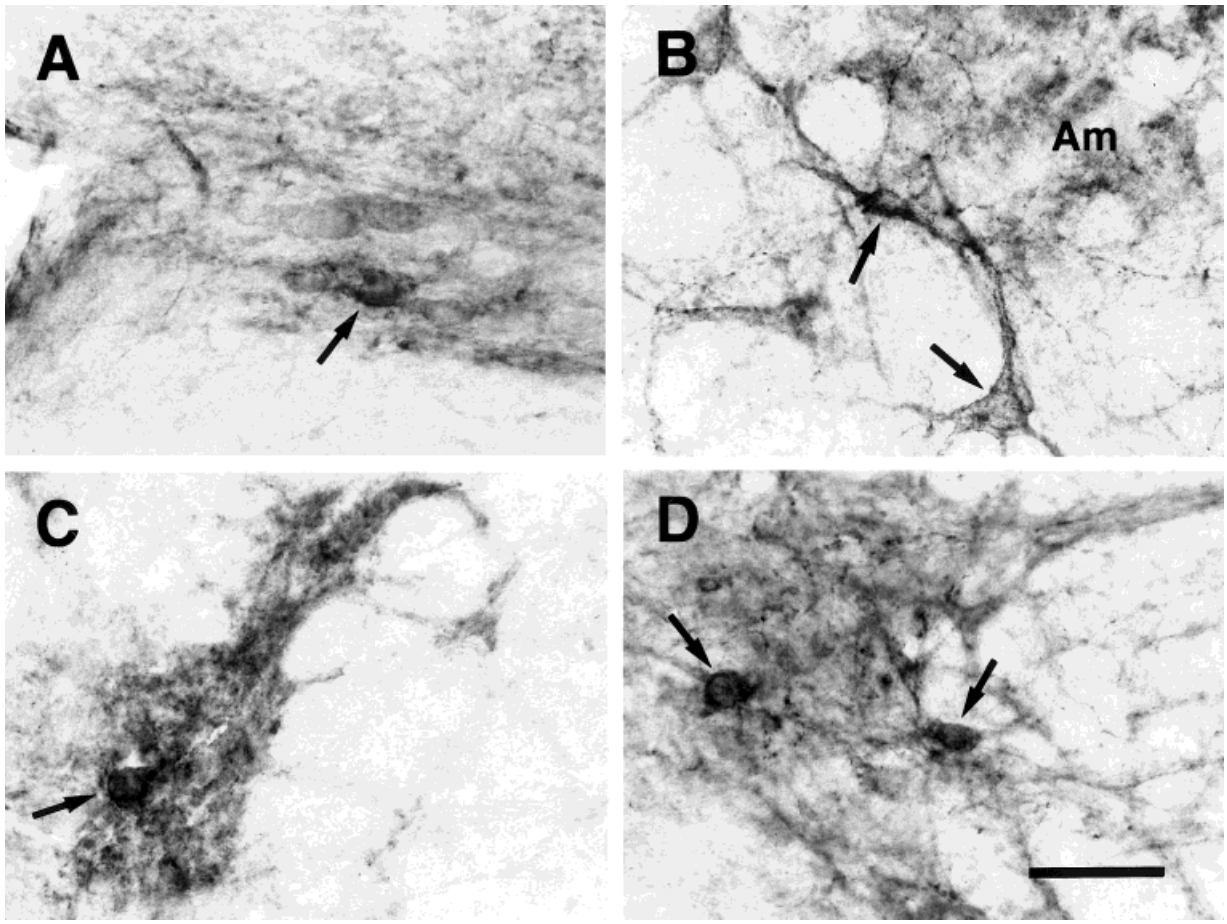

Fig. 14. EP3R-LI in the central autonomic nervous system. **A:** Dorsal motor nucleus of the vagus nerve. **B:** Neuronal cells exhibiting EP3R-LI (arrows) located immediately ventral to the ambiguus nucleus (Am). **C:** Intermediolateral nucleus. **D:** Sacral parasympathetic nucleus. Arrows indicate the neuronal cell bodies that exhibit EP3R-LI. Scale bar = 50 μm.

The thalamus, especially the anterior portion, is the most conspicuous for intense EP3R-LI in the neuropil among the regions examined in the current study, and many neuronal cell bodies in several thalamic nuclei also showed immunoreactivity. However, the roles of EP3R in the thalamus have not yet been discerned. It has been believed that the thalamus is the gateway to the cerebral cortex: It filters and transforms the flow of information from subcortical sites to the cortex (for review, see Sherman and Koch, 1998). The thalamic nuclei that were immunostained strongly belong to the "limbic" or "nonspecific" thalamus. Limbic thalamic nuclei, which include the anterior nuclear group and the mediodorsal nucleus, innervate the limbic cortices and the amygdaloid region. Nonspecific thalamic nuclei contain the intralaminar and midline nuclei, project to widespread areas of the cortex, and terminate in layers other than layer IV, often in layers I and V. This fact is interesting, because the laminar termination pattern matches somewhat the staining pattern in the cortex. Furthermore, the weakly stained thalamic nuclei tend to be the specific relay nuclei that focus their projections on immunonegative layer IV.

The nonspecific thalamic nuclei have been considered to form part of the morphologic substratum of the "ascending activating system," which was assumed to determine the level of consciousness in all its variations from complete alertness and attention to drowsiness and sleep. Many physiologic studies have shown sleep-wake regulation by PGE_2 (for review, see Hayaishi and Matsumura, 1995). Although the site of action of PGE_2 for the regulation of sleep-wakefulness is known to be in the posterior hypothalamus (Onoe et al., 1992), it also is likely that PGE_2 modulates the ascending activating system through the EP3R in the nonspecific thalamic nuclei and, thereby, affects the sleep-wake states.

Previously, we suggested that the EP3R located in the median preoptic nucleus and the medial preoptic area was involved in fever induction by PGE_2 (Nakamura et al., 1999). The neuronal cell group exhibiting EP3R-LI in these preoptic regions seemed to expand into the lateral septal nucleus. A recent histochemical study in the rat brain showed that an intracerebroventricular injection of lipopolysaccharide, which evoked fever, induced cyclooxygenase-2 in endothelial cells of the blood vessels distributed in the lateral septal nucleus as well as in and around those preoptic regions (Cao et al., 1999). During inflammation, therefore, the PGE_2 produced by the induced synthase may activate the EP3R on the neurons,

which are located not only in those preoptic regions but also in the lateral septal nucleus, and, thus trigger the febrile responses in the CNS. Furthermore, EP3R-LI was observed in the ependyma surrounding the lateral ventricle, the third and fourth ventricles, and the aqueduct. Although the physiologic role of PGE_2 in the ependyma remains unknown, it has been reported that the PGE_2 level in cerebrospinal fluid rose after an administration of pyrogens (Coceani et al., 1988). Thus, it is possible that the PGE_2 in cerebrospinal fluid binds to the EP3R on the surface of ependymal cells to mediate some types of peripheral immune stimuli to the CNS.

Synaptic localization of EP3R

Many pharmacologic studies have indicated that EP3R functions as a presynaptic receptor (Mantelli et al., 1991; Molderings et al., 1992, 1994; Exner and Schlicker, 1995; Reinheimer et al., 1998; Spicuzza et al., 1998). From the above-mentioned results of the dorsal rhizotomy experiments, it is inferred that the EP3R protein in the spinal dorsal horn is supplied through axons from dorsal root ganglion cells and is located on the presynaptic membrane. In the current study, EP3R-LI was found in the neuropil of some regions in which the expression of EP3R mRNA has not been reported, such as the superior colliculus and the nucleus of the solitary tract. We believe that these regions also contain presynaptic EP3R protein that originates from the primary sensory neurons that project into the regions. In the compact part of the dorsomedial hypothalamic nucleus, intense EP3R-LI was observed in the neuropil, but immunostained cell bodies were not detected. EP3R mRNA-expressing neurons were distributed broadly in the nucleus (Sugimoto et al., 1994). It is possible that the EP3R-expressing neurons in the nucleus project the axons into the compact part and that the receptor protein from the neurons is accumulated on the axon terminals. On the other hand, neuronal cell bodies and dendrites were immunostained in some other regions, such as the thalamus, medial preoptic area, raphe nuclei, and locus coeruleus. Therefore, EP3R appears to be located on postsynaptic membrane as well as presynaptic membrane. Immunoelectron microscopic analysis would certify the synaptic localization of the receptor protein and provide us with important information on the mechanisms for the synaptic functions of EP3R.

EP3R isoforms and functional significance

The antibody used in the current study was raised against a common portion to three alternatively spliced isoforms—EP3α, EP3β, and EP3γ—which are different only in their C-terminal tails (Takeuchi et al., 1993, 1994; Kitanaka et al., 1996). Immunohistochemical analyses using antibodies against the distinctive portions of the EP3R isoforms would reveal isoform-specific distribution patterns. Recently, it was shown with metabotropic glutamate receptors that axon/dendrite targeting of the receptors was determined by their C-terminal domains (Stowell and Craig, 1999). We believe that, as discussed above, EP3R works as both a presynaptic receptor and a postsynaptic receptor and that it may have different synaptic regulatory mechanisms suitable for its location. These distinct synaptic localizations and functions of EP3R may be ascribed to the spliced isoforms. In other words, each isoform may show its specific synaptic localization and function.

We have cloned complementary DNAs of four bovine EP3R isoforms—EP3A, EP3B, EP3C, and EP3D—and have shown that they are coupled to different G-proteins in a nonneuronal cell line (Namba et al., 1993). This indicates the possibility that the EP3R isoforms regulate synaptic transmission through different intracellular signaling pathways in the nervous system. We recently reported that the EP3B receptor was involved in the regulation of neurotransmitter release by a novel mechanism. Activation of the receptor inhibited dopamine release from a neuroendocrine cell line without affecting Ca^{2+} mobilization in the cells, suggesting that the EP3B receptor-mediated inhibition of neurotransmitter release may be caused at a step after the Ca^{2+} mobilization, such as fusion of secretory granules and plasma membrane (Nakamura et al., 1998). Further studies may reveal the other various mechanisms for the synaptic modulation mediated by the EP3R isoforms.

CONCLUSIONS

This is the first study on overall distribution of PGE receptor proteins in the nervous system. EP3R-LI was observed in various regions, and its distribution suggested unknown CNS functions of EP3R, such as modulation of the noradrenergic and serotonergic monoamine systems. The results of this study also imply the involvement of EP3R in many physiologic actions of various nervous systems, such as autonomic control of homeostasis, somatic and visceral sensations, olfaction, vision, and fever induction. Taken together, these results imply that EP3R may play modulatory roles in "central-peripheral transmission." Furthermore, other unidentified functions of EP3R may be discovered by future studies in light of the results shown in this study. The documented distribution of EP3R will contribute to a further understanding of the diverse actions of PGE_2 in the central and peripheral nervous systems.

ACKNOWLEDGMENTS

The authors are grateful to Drs. Satoshi Tanaka, Yun-Qing Li, and Jin-Lian Li for their helpful technical advice and to Mr. Akira Uesugi for his photographic support. This work was supported in part by grants in aid for Scientific Research from the Ministry of Education, Science, Sports, and Culture of Japan. K.N. is the recipient of a research fellowship from the Japan Society for the Promotion of Science for Young Scientists.

LITERATURE CITED

Aston-Jones G, Chiang C, Alexinsky T. 1991. Discharge of noradrenergic locus coeruleus neurons in behaving rats and monkeys suggests a role in vigilance. Progr Brain Res 88:501–520.

Beiche F, Klein T, Nüsing R, Neuhuber W, Goppelt-Struebe M. 1998. Localization of cyclooxygenase-2 and prostaglandin E_2 receptor EP3 in the rat lumbar spinal cord. J Neuroimmunol 89:26–34.

Bieger D, Hopkins DA. 1987. Viscerotopic representation of the upper alimentary tract in the medulla oblongata in the rat: the nucleus ambiguus. J Comp Neurol 262:546–562.

Blatteis CM, Sehic E. 1998. Cytokines and fever. Ann NY Acad Sci 840: 608–618.

Breder CD, Smith WL, Raz A, Masferrer J, Seibert K, Needleman P, Saper CB. 1992. Distribution and characterization of cyclooxygenase immunoreactivity in the ovine brain. J Comp Neurol 322:409–438.

Breder CD, Dewitt D, Kraig RP. 1995. Characterization of inducible cyclooxygenase in rat brain. J Comp Neurol 355:296–315.

Cao C, Matsumura K, Ozaki M, Watanabe Y. 1999. Lipopolysaccharide injected into the cerebral ventricle evokes fever through induction of cyclooxygenase-2 in brain endothelial cells. J Neurosci 19:716–725.

Chen MCY, Amirian DA, Toomey M, Sanders MJ, Soll AH. 1988. Prostanoid inhibition of canine parietal cells: mediation by the inhibitory guanosine triphosphate-binding protein of adenylate cyclase. Gastroenterology 94:1121–1129.

Coceani F, Lees J, Bishai I. 1988. Further evidence implicating prostaglandin E_2 in the genesis of pyrogen fever. Am J Physiol 254:R463–R469.

Ek M, Kurosawa M, Lundeberg T, Ericsson A. 1998. Activation of vagal afferents after intravenous injection of interleukin-1β: role of endogenous prostaglandins. J Neurosci 18:9471–9479.

Elmquist JK, Scammell TE, Saper CB. 1997. Mechanisms of CNS response to systemic immune challenge: the febrile response. Trends Neurosci 20:565–570.

Exner HJ, Schlicker E. 1995. Prostanoid receptors of the EP3 subtype mediate the inhibitory effect of prostaglandin E_2 on noradrenaline release in the mouse brain cortex. Naunyn-Schmied Arch Pharmacol 351:46–52.

Ferreira SH. 1972. Prostaglandins, aspirin-like drugs and analgesia. Nature New Biol 240:200–203.

Ferreira SH, Moncada S, Vane JR. 1973. Prostaglandins and the mechanism of analgesia produced by aspirin-like drugs. Br J Pharmacol 49:86–97.

Ferreira SH, Nakamura M, de Abreu Castro MS. 1978. The hyperalgesic effects of prostacyclin and prostaglandin E_2. Prostaglandins 16:31–37.

Foote SL, Berridge CW, Adams LM, Pineda JA. 1991. Electrophysiological evidence for the involvement of the locus coeruleus in alerting, orienting, and attending. Progr Brain Res 88:521–532.

Fujimoto N, Kaneko T, Eguchi N, Urade Y, Mizuno N, Hayaishi O. 1992. Biochemical and immunohistochemical demonstration of a tightly bound form of prostaglandin E_2 in the rat brain. Neuroscience 49:591–606.

Garcia-Perez A, Smith WL. 1984. Apical-basolateral membrane asymmetry in canine cortical collecting tubule cells. J Clin Invest 74:63–74.

Hayaishi O, Matsumura H. 1995. Prostaglandins and sleep. Adv Neuroimmunol 5:211–216.

Hebert TE, Moffett S, Morello J-P, Loisel TP, Bichet DG, Barret C, Bouvier M. 1996. A peptide derived from a β_2-adrenergic receptor transmembrane domain inhibits both receptor dimerization and activation. J Biol Chem 271:16384–16392.

Huang C, Tai H-H. 1998. Prostaglandin E_2 receptor EP3α subtype: the role of *N*-glycosylation in ligand binding as revealed by site-directed mutagenesis. Prostaglandins Leukotrienes Essential Fatty Acids 59:265–271.

Ji TH, Grossmann M, Ji I. 1998. G protein-coupled receptors. I. Diversity of receptor-ligand interactions. J Biol Chem 273:17299–17302.

Kitanaka J, Hashimoto H, Gotoh M, Kondo K, Sakata K, Hirasawa Y, Sawada M, Suzumura A, Marunouchi T, Matsuda T, Baba A. 1996. Expression pattern of messenger RNAs for prostanoid receptors in glial cell cultures. Brain Res 707:282–287.

Krall JF, Barrett JD, Jamgotchian N, Korenman SG. 1984. Interaction of prostaglandin E_2 and β-adrenergic catecholamines in the regulation of uterine smooth muscle motility and adenylate cyclase in the rat. J Endocrinol 102:329–336.

Kumazawa T, Mizumura K, Koda H. 1993. Involvement of EP3 subtype of prostaglandin E receptors in PGE_2-induced enhancement of the bradykinin response of nociceptors. Brain Res 632:321–324.

Mantelli L, Amerini S, Rubino A, Ledda F. 1991. Prejunctional prostanoid receptors on cardiac adrenergic terminals belong to the EP3 subtype. Br J Pharmacol 102:573–576.

Matsumura K, Watanabe Y, Onoe H, Watanabe Y, Hayaishi O. 1990. High density of prostaglandin E_2 binding sites in the anterior wall of the 3rd ventricle: a possible site of its hyperthermic action. Brain Res 533:147–151.

Matsumura K, Watanabe Y, Imai-Matsumura K, Connolly M, Koyama Y, Onoe H, Watanabe Y. 1992. Mapping of prostaglandin E_2 binding sites in rat brain using quantitative autoradiography. Brain Res 581:292–298.

Matsumura K, Watanabe Y, Onoe H, Watanabe Y. 1995. Prostacyclin receptor in the brain and central terminals of the primary sensory neurons: an autoradiographic study using a stable prostacyclin analogue [^{3}H]iloprost. Neuroscience 65:493–503.

Minami T, Nishihara I, Uda R, Ito S, Hyodo M, Hayaishi O. 1994. Characterization of EP-receptor subtypes involved in allodynia and hyperalgesia induced by intrathecal administration of prostaglandin E_2 to mice. Br J Pharmacol 112:735–740.

Mohrland JS, Gebhart GF. 1980. Effect of selective destruction of serotonergic neurons in nucleus raphe magnus on morphine-induced antinociception. Life Sci 27:2627–2632.

Molderings G, Malinowska B, Schlicker E. 1992. Inhibition of noradrenaline release in the rat vena cava via prostanoid receptors of the EP3-subtype. Br J Pharmacol 107:352–355.

Molderings GJ, Colling E, Likungu J, Jakschik J, Göthert M. 1994. Modulation of noradrenaline release from the sympathetic nerves of the human saphenous vein and pulmonary artery by presynaptic EP3- and DP-receptors. Br J Pharmacol 111:733–738.

Momiyama T, Todo N, Sugimoto Y, Ichikawa A, Narumiya S. 1996. Membrane depolarization by activation of prostaglandin E receptor EP3 subtype of putative serotonergic neurons in the dorsal raphe nucleus of the rat. Naunyn-Schmied Arch Pharmacol 353:377–381.

Nakamura K, Katoh H, Ichikawa A, Negishi M. 1998. Inhibition of dopamine release by prostaglandin EP3 receptor via pertussis toxin-sensitive and -insensitive pathways in PC12 cells. J Neurochem 71: 646–652.

Nakamura K, Kaneko T, Yamashita Y, Hasegawa H, Katoh H, Ichikawa A, Negishi M. 1999. Immunocytochemical localization of prostaglandin EP3 receptor in the rat hypothalamus. Neurosci Lett 260:117–120.

Namba T, Sugimoto Y, Negishi M, Irie A, Ushikubi F, Kakizuka A, Ito S, Ichikawa A, Narumiya S. 1993. Alternative splicing of C-terminal tail of prostaglandin E receptor subtype EP3 determines G-protein specificity. Nature 365:166–170.

Negishi M, Sugimoto Y, Ichikawa A. 1995. Molecular mechanisms of diverse actions of prostanoid receptors. Biochim Biophys Acta 1259: 109–120.

Nimchinsky EA, Hof PR, Janssen WGM, Morrison JH, Schmauss C. 1997. Expression of dopamine D_3 receptor dimers and tetramers in brain and in transfected cells. J Biol Chem 272:29229–29237.

Ojeda SR, Negro-Vilar A, McCann SM. 1982. Evidence for involvement of α-adrenergic receptors in norepinephrine-induced prostaglandin E_2 and luteinizing hormone-releasing hormone release from the median eminence. Endocrinology 110:409–412.

Oka T, Hori T, Hosoi M, Oka K, Abe M, Kubo C. 1997. Biphasic modulation in the trigeminal nociceptive neuronal responses by the intracerebroventricular prostaglandin E_2 may be mediated through different EP receptors subtypes in rats. Brain Res 771:278–284.

Onoe H, Watanabe Y, Ono K, Koyama Y, Hayaishi O. 1992. Prostaglandin E_2 exerts an awaking effect in the posterior hypothalamus at a site distinct from that mediating its febrile action in the anterior hypothalamus. J Neurosci 12:2715–2725.

Paxinos G, Watson C. 1998. The rat brain in stereotaxic coordinates, 4th ed. San Diego: Academic Press.

Reinheimer T, Harnack E, Racke K, Wessler I. 1998. Prostanoid receptors of the EP3 subtype mediate inhibition of evoked [^{3}H]acetylcholine release from isolated human bronchi. Br J Pharmacol 125:271–276.

Richelsen B, Beck-Nielsen H. 1984. Decrease of prostaglandin E_2 receptor binding is accompanied by reduced antilipolytic effects of prostaglandin E_2 in isolated rat adipocytes. J Lipid Res 26:127–134.

Scaramuzzi OE, Baile CA, Mayer J. 1971. Prostaglandins and food intake of rats. Experientia 27:256–257.

Sefton AJ, Dreher B. 1995. Visual system. In: Paxinos G, editor: The rat nervous system, 2nd ed. San Diego: Academic Press. p 833–898.

Sherman SM, Koch C. 1998. Thalamus. In: Shepherd GM, editor: The synaptic organization of the brain. New York: Oxford University Press. p 289–328.

Spicuzza L, Giembycz MA, Barnes PJ, Belvisi MG. 1998. Prostaglandin E_2 suppression of acetylcholine release from parasympathetic nerves innervating guinea-pig trachea by interacting with prostanoid receptors of the EP3-subtype. Br J Pharmacol 123:1246–1252.

Steinbusch HWM. 1981. Distribution of serotonin-immunoreactivity in the central nervous system of the rat-cell bodies and terminals. Neuroscience 6:557–618.

Stitt JT. 1986. Prostaglandin E as the neural mediator of the febrile response. Yale J Biol Med 59:137–149.

Stowell JN, Craig AM. 1999. Axon/dendrite targeting of metabotropic

glutamate receptors by their cytoplasmic carboxy-terminal domains. Neuron 22:525–536.

Sugimoto Y, Shigemoto R, Namba T, Negishi M, Mizuno N, Narumiya S, Ichikawa A. 1994. Distribution of the messenger RNA for the prostaglandin E receptor subtype EP3 in the mouse nervous system. Neuroscience 62:919–928.

Taiwo YO, Levine JD. 1988. Prostaglandins inhibit endogenous pain control mechanisms by blocking transmission at spinal noradrenergic synapses. J Neurosci 8:1346–1349.

Takeuchi K, Abe T, Takahashi N, Abe K. 1993. Molecular cloning and intrarenal localization of rat prostaglandin E_2 receptor EP3 subtype. Biochem Biophys Res Commun 194:885–891.

Takeuchi K, Takahashi N, Abe T, Abe K. 1994. Two isoforms of the rat kidney EP3 receptor derived by alternative RNA splicing: intrarenal expression co-localization. Biochem Biophys Res Commun 199: 834–840.

Törk I. 1985. Raphe nuclei and serotonin containing systems. In: Paxinos G, editor: The rat nervous system, vol 2. North Ryde: Academic Press. p 43–78.

Uda R, Horiguchi S, Ito S, Hyodo M, Hayaishi O. 1990. Nociceptive effects induced by intrathecal administration of prostaglandin D_2, E_2, or $F_{2\alpha}$ to conscious mice. Brain Res 510:26–32.

Ushikubi F, Segi E, Sugimoto Y, Murata T, Matsuoka T, Kobayashi T, Hizaki H, Tuboi K, Katsuyama M, Ichikawa A, Tanaka T, Yoshida N, Narumiya S. 1998. Impaired febrile response in mice lacking the prostaglandin E receptor subtype EP3. Nature 395:281–284.

Vasko MR, Pang I-H, Vogt M. 1984. Involvement of 5-hydroxytryptamine-containing neurons in antinociception produced by injection of morphine into nucleus raphe magnus or onto spinal cord. Brain Res 306:341–348.

Vilhardt H, Hedqvist P. 1970. A possible role of prostaglandin E_2 in the regulation of vasopressin secretion in rats. Life Sci 9:825–830.

Watanabe Y, Watanabe Y, Hayaishi O. 1988. Quantitative autoradiographic localization of prostaglandin E_2 binding sites in monkey diencephalon. J Neurosci 8:2003–2010.

Yamagata K, Andreasson KI, Kaufmann WE, Barnes CA, Worley PF. 1993. Expression of a mitogen-inducible cyclooxygenase in brain neurons: regulation by synaptic activity and glucocorticoids. Neuron 11:371–386.

Yokotani K, Okuma Y, Osumi Y. 1996. Inhibition of vagally mediated gastric acid secretion by activation of central prostanoid EP3 receptors in urethane-anaesthetized rats. Br J Pharmacol 117:653–656.

Zhang J, Rivest S. 1999. Distribution, regulation and colocalization of the genes encoding the EP2- and EP4-PGE_2 receptors in the rat brain and neuronal responses to systemic inflammation. Eur J Neurosci 11:2651–2668.

Zhao C, Shichi H. 1995. Immunocytochemical localization of prostaglandin E_2 receptor subtypes in porcine ocular tissues. II. Nonuveal tissues. J Ocul Pharmacol Ther 11:437–445.